Received: 12 June 2025 | Revised: 21 January 2026 | Accepted: 19 February 2026

DOI: 10.1002/ecm.70058

METHOD

ECOLOGICAL MONOGRAPHS
ECOLOGICAL SOCIETY OF AMERICA

Going round in cycles but going somewhere: Deciphering cyclical dynamics using Ecological Trajectory Analysis

Nicolas Djeghri[1] | **Anthony Sturbois**[1,2] | **Pierre Hélaouët**[3] | **Quentin Geissmann**[4] | **Peggy Rimmelin-Maury**[5] | **Aurélien Boyé**[6] | **Olivier Gauthier**[1,5] | **Miquel De Cáceres**[7]

[1]Univ Brest, CNRS, IRD, Ifremer, UMR6539 LEMAR, Plouzané, France

[2]Vivarmor Nature, Réserve naturelle de la Baie de Saint-Brieuc, Hillion, France

[3]Marine Biological Association, Continuous Plankton Recorder Survey, Plymouth, UK

[4]Center for Quantitative Genetics and Genomics, Aarhus University, Aarhus, Denmark

[5]Univ Brest, CNRS, IRD, UAR3113 OSU IUEM, Plouzané, France

[6]Ifremer, Laboratory of Coastal Benthic Ecology, Plouzané, France

[7]CREAF-CSIC, E-08193, Bellaterra, Catalonia, Spain

Correspondence
Nicolas Djeghri
Email: nicolas.djeghri@univ-brest.fr

Funding information
ISblue project, Interdisciplinary graduate school for the blue planet, Grant/Award Number: ANR-17-EURE-0015; French government under the program "Investissements d'Avenir" embedded in France 2030

Handling Editor: Chuliang Song

Abstract

Earth's ecological dynamics are largely rhythmic, tied to regular cycles such as seasons, lunar phases, days, or tides. Subdisciplines of ecology such as phenology have developed specific concepts and metrics adapted to describe and analyze cyclical dynamics, but they operate in a largely unidimensional framework. There is therefore a lack of suitable tools for describing cyclical ecological dynamics in multidimensional spaces. Here, we introduce Cyclical Ecological Trajectory Analysis (CETA), an extension of Ecological Trajectory Analysis, allowing for describing and comparing cyclical dynamics in a multidimensional context without dimensionality reduction. CETA provides metrics to quantify cycles' geometry and resemblance in a multidimensional space of interest and offers a multidimensional equivalent of the concept of phenological advance and delays. We provide four ecological examples demonstrating how CETA can be useful to study different cyclical dynamics (seasons, days, tides), using different data (community composition, environmental data) and in different contexts (observational or experimental). We also show how CETA can be articulated with methods of multiscale analysis for time series. We conclude by summarizing the advantages and limitations of the method, its wide range of potential applications, as well as its connections and synergies with other, already available, aspects of the Ecological Trajectory Analysis framework.

KEYWORDS

beta diversity, chronobiology, community dynamics, diel cycle, distance matrices, Ecological Trajectory Analysis, multivariate statistics, phenology, seasonality, temporal dynamics

INTRODUCTION

Time is most often thought of as linear, future flowing into past through present. In ecology, however, it can sometimes be useful to also consider time as cyclical (or recurrent, Post, 2019). Cyclical time in ecology is dictated by the astronomical movements of the Earth, Sun, and Moon that imprint strong but largely predictable rhythmic forcings (seasons, diel cycles, lunar cycles, tides…) on organisms, communities, and ecosystems. Because of those strong but predictable changes, organisms evolved ways to keep track of cyclical time through internal clocks and external environmental cues (Helm et al., 2017; Park & Post, 2022), helping them to forecast and time adapted responses to cyclic forcings. Examples include migration of birds (Åkesson et al., 2017), diapause in zooplankton (Wilson et al., 2016) or flowering in plants (Kudoh, 2016) timed with seasons, as well as diel (Gaston, 2019) or tidal (Bulla et al., 2017) activity patterns in animals. Individual responses then transfer across the ecological levels of organization to populations, communities, and ecosystems, making the functioning of Earth ecosystems itself largely rhythmic: Seasonal greening patterns—correlated with ecosystem productivity and biomass—are visible from space (Behrenfeld, 2014; Piao et al., 2019); differences in biological activity at night and day affect the cycling of elements (Cox & Gaston, 2024; Steinberg & Landry, 2017). Cyclical dynamics have important repercussions for fundamental ecological questions such as co-existence theory (Rudolf, 2019) or latitudinal biodiversity gradients (Ghalambor et al., 2006; Janzen, 1967). Finally, under increasing anthropogenic pressures—from artificial light at night to climate change—many cyclical ecological dynamics have changed dramatically in the last few decades (Behrenfeld, 2014; Cox & Gaston, 2024; Piao et al., 2019), making alteration to cyclical dynamics a central aspect of how humans affect the biosphere and a key object of study for ecologists.

Despite their prominent role in shaping Earth's ecology, there is concern that cyclical dynamics are not accounted often enough (Gaston, 2019; White & Hastings, 2020; Yang, 2020). We believe an important hurdle lies with the statistical frameworks at our disposal to describe cyclical dynamics, particularly in a multidimensional context. Good examples are phenological metrics which often consist of timings of specific biological or ecological events. These events may be directly observed and their timing recorded as in the classic case of the blossom of Kyoto's cherry trees (Aono & Kazui, 2008, see many more examples in Schwartz, 2013). Alternatively, the timing of events may be extracted (as well as other descriptive statistics) from higher frequency signals as is done to identify the timing of the seasonal chlorophyll peak in the oceans (Ferreira et al., 2014). These descriptive methods apply to unidimensional data and are not straightforwardly translated in a multidimensional context (i.e., the notion of peak has little sense in a multidimensional context). This may present an important problem when one wants to extract phenological metrics from objects that are intrinsically multidimensional, such as, among others, ecological communities (see also Inouye et al., 2019). Hence, generalizing ecological concepts relevant to univariate cyclical data to multidimensional context could help improve integration and synthesis across some of ecology subdisciplines—such as phenology and community ecology—by giving them more common ground. More practically, this would also promote a better understanding of cyclical ecological dynamics and of how they are transformed by anthropogenic pressures.

With the aim to design a new statistical tool for the multidimensional description of cyclical ecological dynamics, we build and expand on the existing framework of Ecological Trajectory Analysis (ETA, previously Community Trajectory Analysis, CTA). ETA is a statistical and data visualization framework originally developed for community ecology (De Cáceres et al., 2019) that approaches ecological temporal dynamics as trajectories embedded in an *n*-dimensional space. ETA employs a geometric approach to describe individual trajectories (directionality, turning angles, shapes) and to assess the similarity between pairs of ecological trajectories opening the possibility to not only compare ecological states, but also ecological dynamics, while preserving their full dimensionality. Ecological processes may then be inferred from the geometric properties of trajectories (e.g., a trajectory with high directionality may hint at a strong underlying selective process sensu Vellend, 2016), complementing other approaches to relate patterns and processes (Ovaskainen et al., 2019). The original ETA framework has gained interest among ecologists and grows rapidly with extensions allowing taking into account baselines or reference ecological states (Sturbois et al., 2021, 2023), generalization outside of community ecology (Sturbois et al., 2022), or methods to identify ecological dynamic regimes (Sánchez-Pinillos et al., 2023). ETA has been used to reveal habitat-dependent community dynamics in coastal macrobenthos (Toumi et al., 2023), to study the effect of disturbance and nutrient enrichment on grassland succession (DeSiervo et al., 2023), or to experimentally assess the effect of predator mass mortality events on freshwater food webs (Tye et al., 2024).

CETA, the cyclical extension of ETA presented here, proceeds by first defining trajectories adapted to the exploration of cyclical dynamics. Then, metrics specifically describing the properties and the similarity between these trajectories can be computed. CETA also provides a multidimensional generalization of the phenological concept of advances and delays. We illustrate our framework by presenting examples of applications of CETA on different communities (birds, zooplankton, insects) focusing on different timescales (seasonal, circadian) and under both observational and experimental contexts. We conclude with a last example using high-frequency marine environmental data with intertwined cyclical dynamics

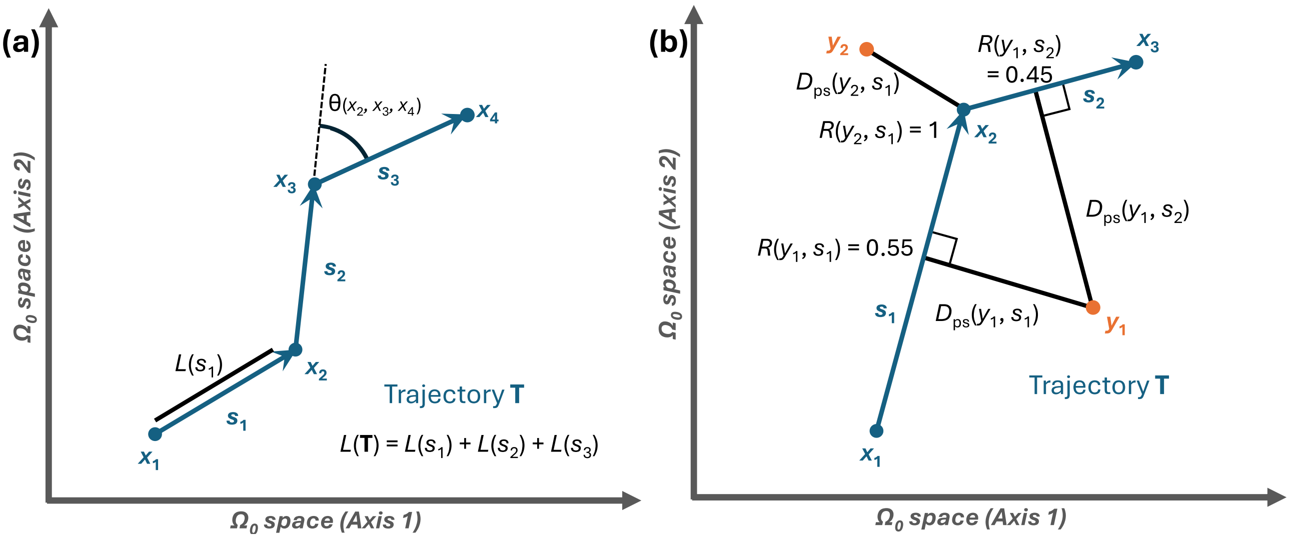

FIGURE 1 Graphical illustration of some of the original ecological trajectory analysis metrics (De Cáceres et al., 2019). (a) Segment length $L(s)$ and trajectory path length $L(\mathbf{T})$, change of direction between segments θ, and (b) point-to-segment and point-to-trajectory distances (D_{ps} and D_{pt}) as well as relative position of a point along a segment $R(y, s)$.

(seasonal, tidal) to show how CETA can be articulated with multiscale analysis methods able to model complex temporal signals (e.g., temporal eigenfunction analysis, Legendre & Gauthier, 2014).

ETA FRAMEWORK

Before proceeding to the description of Cyclical Ecological Trajectory Analysis (CETA) itself, we give a summary of the metrics and concepts of the ETA framework (De Cáceres et al., 2019; Sturbois et al., 2022) essential to understanding CETA.

Let $o_1, o_2, ..., o_n$ be a time-ordered set of ecological observations associated to ordered times $t_1, t_2, ..., t_n$. For all i in $\{1, 2, ..., n\}$, let $\boldsymbol{x}_i$ contain the ecological states corresponding to o_i in a chosen multidimensional space Ω_0. Ω_0 is defined by the set of ecosystem properties of interest and is computed from a distance matrix of pairwise dissimilarity coefficients d (e.g., the percentage difference or Bray–Curtis coefficient, Bray & Curtis, 1957). The choice of representing Ω_0 using a distance matrix, as opposed to a rectangular matrix, allows accommodating flexibly the wealth of resemblance metrics potentially useful in ecology (Legendre & De Cáceres, 2013; Ricotta, 2021). An ecological trajectory of size n is defined as the sequence of time-ordered ecological states $\mathbf{T} = \{(\boldsymbol{x}_1, t_1), (\boldsymbol{x}_2, t_2), ..., (\boldsymbol{x}_n, t_n)\}$. Alternatively, $\mathbf{T}$ can be defined as the set of $n - 1$ directed segments $s_i = \{\boldsymbol{x}_i, \boldsymbol{x}_{i+1}\}$ corresponding to consecutive time intervals $\{t_i, t_{i+1}\}$.

The existing ETA framework (De Cáceres et al., 2019; Sturbois et al., 2021, 2023) allows to describe and compare ecological trajectories and is based on the computation of different length- and direction-based metrics calculated using the full Ω_0 space (i.e., without dimension reduction):

1. $L(s_i)$ and $L(\mathbf{T})$: segment length and trajectory path length (Figure 1a).
2. $\theta_{ijk}(\boldsymbol{x}_i, \boldsymbol{x}_j, \boldsymbol{x}_k)$: change of direction (0° < θ < 180°) of vector $\overrightarrow{\boldsymbol{x}_j\boldsymbol{x}_k}$ with respect to vector $\overrightarrow{\boldsymbol{x}_i\boldsymbol{x}_j}$ in the triangle defined by the points $\boldsymbol{x}_i$, $\boldsymbol{x}_j$ and $\boldsymbol{x}_k$ (Figure 1a) using trigonometric rules. It can also be expressed as the turning angle between segments $s_i = \{\boldsymbol{x}_i, \boldsymbol{x}_j\}$ and $s_j = \{\boldsymbol{x}_j, \boldsymbol{x}_k\}$.
3. $D_{ps}(y, s_i)$ and $D_{pt}(y, \mathbf{T})$: the distance between ecological state y of Ω_0 and segment s_i or trajectory $\mathbf{T}$ (obtained by orthogonal projection, Figure 1b). $D_{pt}(y, \mathbf{T}) = \min(D_{ps}(y, s_i))$ with s_i the segments constituting $\mathbf{T}$.
4. $R(y, s_i)$ and $R(y, \mathbf{T})$: the relative position (varying between 0 and 1) of point y on segment s_i or a trajectory $\mathbf{T}$ after orthogonal projection (Figure 1b).
5. $D_{DSP}(\mathbf{T_1}, \mathbf{T_2})$ and $D_{SDSP}(\mathbf{T_1}, \mathbf{T_2})$: the geometric resemblance between pairs of trajectories. Respectively, the directed segment path dissimilarity and the symmetrized directed segment path dissimilarity measure dissimilarity between trajectories $\mathbf{T_1}$ and $\mathbf{T_2}$, taking into account their positions, shapes, sizes, and directions. $D_{DSP}(\mathbf{T_1}, \mathbf{T_2})$ and $D_{SDSP}(\mathbf{T_1}, \mathbf{T_2})$ are based on modifications of the Hausdorff distance allowing us to

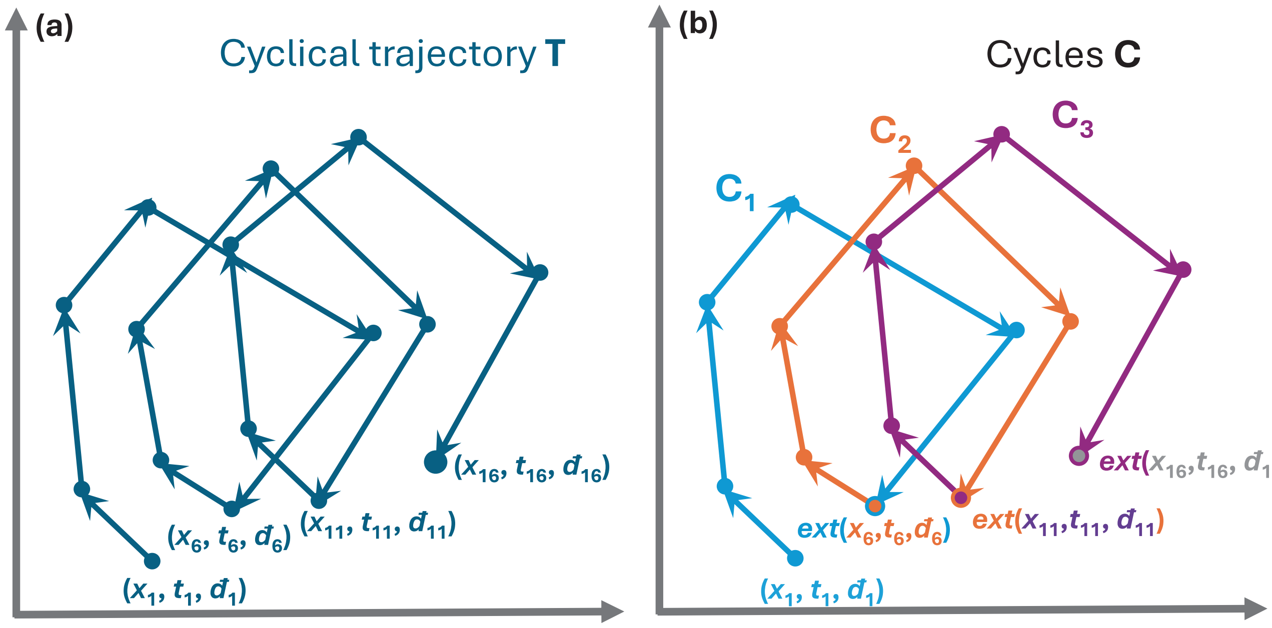

FIGURE 2 Graphical illustration of a cyclical trajectory **T** (a) and cycles $\mathbf{C_1}$, $\mathbf{C_2}$, and $\mathbf{C_3}$ that can be defined within **T** (b). This scenario illustrates a regular sampling where the cycles can always be set to start at sampled times ($\boldsymbol{x}_1$, $\boldsymbol{x}_6$, and $\boldsymbol{x}_{11}$). The date at the start and end of the cycles and duration of cycles are equal (i.e., $đ_1 = đ_6 = đ_{11} = đ_{16}$, and $\text{DUR}_\text{C} = t_6 - t_1 = t_{11} - t_6 = t_{16} - t_{11}$). Because the cycles are consecutive, they share some ecological states represented as bicolor points (inner color = color of the cycle within which the point is not external, outer color = color of the cycle within which the point is external).

take into account direction. Once pairwise dissimilarities between trajectories are obtained, it is possible to represent the trajectories in a new multidimensional space (the "trajectory space," Ω_T) through principal coordinates analysis (PCoA). Note that it is possible to center trajectories $\mathbf{T_1}$ and $\mathbf{T_2}$ before computing $D_\text{DSP}(\mathbf{T_1}, \mathbf{T_2})$ and $D_\text{SDSP}(\mathbf{T_1}, \mathbf{T_2})$ so that position does not affect dissimilarity computations.

The ETA metrics presented here, alongside more derived ones (see De Cáceres et al., 2019; Sturbois et al., 2021) can be interpreted ecologically. For instance, high $L(s_i)$ or $L(\mathbf{T})$ imply important ecological change, whereas near zero θ_{ijk} implies that two consecutive segments are oriented in the same direction meaning that they are changing along the same axes (e.g., same increasing or decreasing species). Measured geometric resemblance between pairs of trajectories $D_\text{DSP}(\mathbf{T_1}, \mathbf{T_2})$ or $D_\text{SDSP}(\mathbf{T_1}, \mathbf{T_2})$ can be interpreted as resemblance of ecological dynamics.

CYCLICAL ECOLOGICAL TRAJECTORY ANALYSIS

CETA aims to extend ETA, allowing description and comparison of cyclical dynamics such as seasonal or diel. In doing so, we define three specific types of ecological trajectories: cyclical trajectories, cycles, and fixed-date trajectories. Importantly, CETA does not aim to detect cyclical dynamics. These must be known a priori or detected from the data using methods outside of CETA (as exemplified in our ecological application on tidal cycles). CETA importantly inherits from ETA its grounding in a multidimensional, dissimilarity-based, Ω_0 space that is fully preserved during computation of CETA metrics.

Definitions

Cyclical Trajectories

We call a "cyclical trajectory" a trajectory **T** of size n displaying cyclical dynamics associated with ecological states $\boldsymbol{x}_i$, times t_i, and dates $đ_i$ (using the symbol $đ$ to differentiate it from d referring to distance, Figure 2a) such as

$$\mathbf{T} = \{(\boldsymbol{x}_1, t_1, đ_1), (\boldsymbol{x}_2, t_2, đ_2), \ldots, (\boldsymbol{x}_n, t_n, đ_n)\} \tag{1}$$

We call DUR_C the duration of a cycle within **T** (e.g., $\text{DUR}_\text{C} \approx 365$ days if the cycles of interest are annual).

A specificity of cyclical trajectories, as compared to non-cyclical trajectories, is the inclusion of dates $đ_i$

representing recurrent, or cyclical, time sensu Post (2019). By contrast, times t_i represent linear time as in non-cyclical trajectories (i.e., the 17th of December recurs every year, in that sense, we call it a date. However, the 17th of December 2009 occurred only once, and BBC radio is grateful). Dates are circular variables, meaning that they loop back to their smallest values when reaching their maximum values, and must be expressed in the same unit as times. Unlike times, different observations can have the same date within **T**. Dates can be computed from times using the modulo (mod) operator:

$$đ_i = (t_i - t_1) \bmod \mathrm{DUR_C} + z, \tag{2}$$

with z an offset value belonging to $[-\mathrm{DUR_C}/2; \mathrm{DUR_C}/2]$, allowing flexibility in the positioning of the start of cycles with respect to times. Our choice of the word "date" reflects our expectation that CETA may most often be used to analyze seasonality. However, this is only a shorthand, and "dates" might become "hours" in the context of a study on diel cycles.

Cycles

When attempting to extract cycles from a given cyclical trajectory, one runs into what we call the "December-to-January segment problem" best described with an example: Consider a multiannual, monthly sampled time series yielding a cyclical trajectory of interest. Describing cycles as sub-trajectories going from the January sampling to the December sampling means systematically leaving out the directed segment connecting December to January. However, defining cycles as sub-trajectories going from January to January of the next year means representing the ecological states associated with January twice in every cycle. None of these approaches are appropriate within ETA as some metrics or operations rely on the concept of directed segment (e.g., trajectory length, D_{SDSP}) whereas others rely on ecological states (e.g., trajectory centering). There is a need for a more flexible concept.

To solve the December-to-January segment problem we introduce the concept of "trajectory section" to ETA (a detailed formal description is given in Appendix S1). Briefly, trajectory sections allow to flexibly cut longer trajectories between two chosen times (t_{start} and t_{end}). Either or both of the first and last ecological states of a trajectory section may be set to be "external" and are used differently for different ETA operations and metrics. External ecological states are included in operations and metrics relying on directed segments (such as trajectory length) but excluded from operations and metrics relying on ecological states (for instance the weight of external ecological states can be set to zero when centering a trajectory section). Moreover, trajectory sections can be defined between any arbitrary times along a trajectory. If these times do not correspond to measured ecological states, interpolated ecological states can be computed (Appendix S1) accommodating irregular sampling (i.e., sampling not performed at regular dates). These interpolated ecological states are always set to external so that they do not impact ecological state-based computations.

In the context of CETA, we define a cycle **C** as a specific type of trajectory section defined within a cyclical trajectory and where $t_{\mathrm{end}} - t_{\mathrm{start}} = \mathrm{DUR_C}$ (Figure 2b). This implies that the dates $đ_{\mathrm{start}}$ and $đ_{\mathrm{end}}$ associated to t_{start} and t_{end} are equal. To avoid inappropriate double counting of the ecological states associated to this date, at least one of the "ends" of cycles is set to external (Figure 2b).

Fixed-date trajectories

Fixed-date trajectories (**fdT**) are sub-trajectories linking the ecological states of equal dates across **T**. For instance, if **T** represents a multiannual monthly sampled time series, there will be 12 **fdT**, the first one linking all ecological states of January months and so on. In the case of regular enough sampling (i.e., sampling at fixed dates each cycle), establishing **fdT** is simple as fixed-date ecological states are readily available. If sampling is irregular, **fdT** might be built out of interpolated ecological states computed for fixed dates, but this entails the risk of misrepresenting their shapes. **fdT** are particularly informative about long-term changes (i.e., changes occurring at longer time scales than $\mathrm{DUR_C}$) at the specific date they represent.

Descriptive metrics for cycles and fixed-date trajectories

All descriptive metrics of trajectories existing within ETA (De Cáceres et al., 2019; Sturbois et al., 2021) are technically applicable to cycles and fixed-date trajectories. However, some might have little or different sense when studying cyclical dynamics. Below we review how existing ETA metrics apply to the type of trajectories studied within CETA and introduce a new metric describing the geometry of cycles.

Describing cycles

Let **C** be a cycle defined within cyclical trajectory **T**. The length of **C**, $L(\mathbf{C})$, informs on the amplitude of the cycle and the amount of ecological variation it represents. The original ETA framework also allows to compute trajectory speed as its length divided by its duration. However, because cycles have by definition a fixed duration, their speed is redundant with their length. In non-cyclical trajectories, length is completed by a metric of directionality (DIR(**T**)) indicative of whether a trajectory is rather straight or windy. This metric is inappropriate for cycles which return near their initial state. We therefore introduce the "convexity" of a cycle, CONV(**C**), as the cyclical analogue of directionality.

Except for the very start and end of **T**, it is possible to associate to each internal ecological state $\boldsymbol{x}_i$ of cycle **C** a change of direction $\theta_i(\boldsymbol{x}_{i-1}, \boldsymbol{x}_\mathrm{i}, \boldsymbol{x}_{i+1})$. The convexity of cycle **C**, CONV(**C**) is computed as

$$\mathrm{CONV}(\mathbf{C}) = \frac{360}{\sum \theta_i}. \tag{3}$$

Cycle convexity relies on the geometric rule that the sum of external angles of a convex polygon in a plane is always equal to 360°. Hence, to go back to where it started, an idealistic simple cycle will have to make at least a 360° directional change in total, yielding a convexity of 1. Cycles presenting concavities and "bends" in more than two dimensions will have greater sums of changes of direction and convexity closer to 0. Ecologically, and provided noise is well controlled (see below), lower convexity will be indicative of higher dimensional, and generally more complex cycles (for instance some variables involved in the cycle may be bimodal, Djeghri et al., 2018; Geissmann et al., 2022), whereas higher convexity is indicative of simpler dynamics. Finally, note that it is technically possible that a cycle has a convexity >1 if it is both very regular and open (i.e., the last ecological state does not return close enough to the first ecological state).

We include in Appendix S2 a study on the behavior of metrics describing cycles under increasing noise using synthetic data. Importantly, this study shows that noise tends to decrease convexity and increase length. Allowing noise to vary in higher dimensions than the dimensions in which the cycles lie produces similar effects. These dependencies were expected as they are also found in the analogous ETA metrics (directionality and trajectory length, De Cáceres et al., 2019) and stem directly from the descriptive nature of the framework.

Describing fixed-date trajectories

Some ETA metrics applied to **fdT** may be of particular interest because these trajectories represent the change in ecological state at fixed dates along ecological cycles. Directionality (De Cáceres et al., 2019) of **fdT** allows tracking parts of ecological cycles that have experienced directional change (i.e., potentially indicative of selection sensu Vellend, 2016). Convergence or divergence (De Cáceres et al., 2019) between **fdT** can inform on part of the cycles becoming more similar or growing dissimilar. This complements the information given by computing cyclical shifts (a way of quantifying cyclical advances and delays in CETA, see below) by being sensitive to long-term changes in position as well as to changes in timing along the cycle.

Resemblance between CETA trajectories, and the Ω_C and Ω_fdT spaces

Resemblance metrics for trajectories (directed segment path dissimilarity and symmetrized directed segment path dissimilarity, De Cáceres et al., 2019) can be computed between any CETA-specific trajectories. Once pairwise resemblances (expressed as dissimilarities) between trajectories of interest have been obtained for all pairs, they define a space Ω_T of resemblance between trajectories that can be represented graphically using PCoA. With CETA, two such spaces are of particular interest: the space of cycles Ω_C, obtained from pairwise distances between cycles, and the space of fixed-date trajectories Ω_fdT, obtained from pairwise distances between fixed-date trajectories.

The cycle space Ω_C

Studying the resemblance between different cycles obtained from one (or more) cyclical trajectory **T** in the Ω_C space has the potential to yield important information on the variability of the cyclical dynamics along a cyclical trajectory. The resemblance between cycles can be visualized in a biplot. Dynamic beta diversity $\mathrm{dBD}_\mathrm{Total}$—a measure of the variation in community dynamics, originally across space (De Cáceres et al., 2019; Legendre & De Cáceres, 2013)—computed in Ω_C gives an indication of how diverse cycles are within one or more trajectories. If (as might often be the case) Ω_C is obtained from many cycles extracted from one cyclical trajectory, $\mathrm{dBD}_\mathrm{Total}$ will be interpreted in terms of temporal rather than spatial dynamic beta diversity. $\mathrm{dBD}_\mathrm{Total}$ can be further decomposed into "Local Contribution to dynamic Beta Diversity" (LCdBD; Legendre & De Cáceres, 2013; De Cáceres et al., 2019). Applied in the Ω_C space, the LCdBD are not really "local contributions" but "individual cycle contributions" to dynamic beta diversity yielding information on how peculiar a cycle is with reference to other cycles in the Ω_C space.

Second-stage trajectory analysis in cycle space Ω_{C}

Extracting cycles from a cyclical trajectory and computing the Ω_{C} space effectively brings one back to the initial condition of application of ETA: a dissimilarity space with time-ordered observations. It is therefore possible to study trajectories inside the Ω_{C} space using the ETA framework (see the North Sea zooplankton ecological example). The geometry of those second-stage trajectories in the Ω_{C} space will be informative on long-term changes in the cyclical dynamics of the system under study. However, an additional analysis (Appendix S3) suggests that in many cases, second-stage trajectories will be very similar to the trajectories joining the centers of cycles and are thus redundant with a simple averaging. Another way to use second-stage trajectories is to base them on centered cycles instead, effectively bringing forth the unique information given by CETA on temporal changes in cycles shapes and sizes irrespective of their positions in the Ω_0 space.

The fixed-date trajectory space Ω_{fdT}

Studying the resemblance between different fixed-date trajectories obtained from one (or more) cyclical trajectory **T** in the Ω_{fdT} space will yield information on similarities between the long-term dynamics of different parts of the cycles. Computing LCdBD (i.e., in this case "local" would refer to the trajectory of a specific date) in the Ω_{fdT} space will yield information on parts of the cycles (i.e., dates) that have had peculiar long-term dynamics and are thus the most responsible for the long-term deformation of the cycles. For the specific goal of assessing which dates changed the most and are thus responsible for long-term change in cycle shapes, it is advisable to center fixed-date trajectories before computing resemblances, removing the effect of position and allowing focus on differences in dynamics (see the insect day-night dynamics example).

Cyclical shifts: Advances and delays

A key contribution of CETA, is to open the possibility to translate the classical phenological question of quantifying differences in timing of an ecological event (e.g., advances or delays) into a multidimensional form, compatible with the data most often used by, among others, community ecologists, and answering recent calls for a more time-explicit community ecology (Inouye et al., 2019; Yang, 2020). We call "cyclical shifts" our multidimensional measures of advances and delays along ecological cycles and define them as follows.

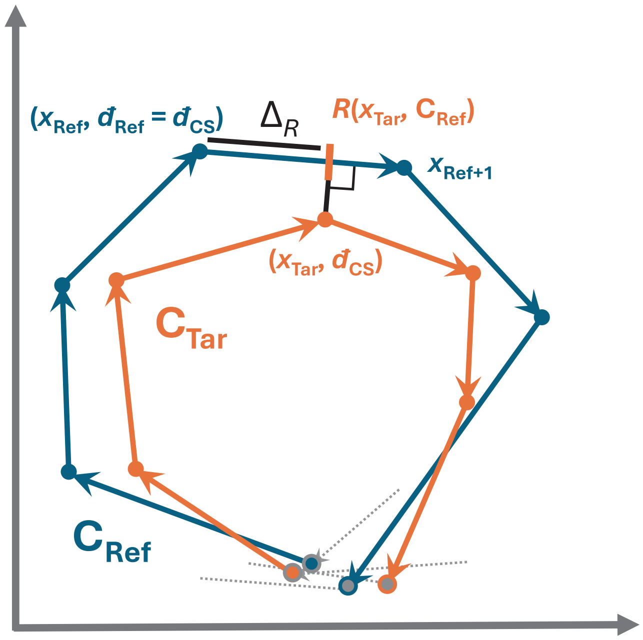

FIGURE 3 Graphical illustration of a cyclical shift in relative position Δ_R between ecological state $\boldsymbol{x}_{\mathrm{CS}}$ associated to date $đ_{\mathrm{CS}}$ belonging to cycle $\mathbf{C}_{\mathbf{Tar}}$ (orange) and $\boldsymbol{x}_{\mathrm{Ref}}$ (with $đ_{\mathrm{Ref}} = đ_{\mathrm{CS}}$) belonging to cycle $\mathbf{C}_{\mathbf{Ref}}$ (blue). This example represents an advance scenario for the date investigated ($đ_{\mathrm{Tar}}$). Both cycles belong to a longer cyclical trajectory **T** (only suggested by the gray dotted lines). The cyclical shift in relative position has an equivalent in time units Δ_t (see text) computed using the segment s_i onto which the projection of $\boldsymbol{x}_{\mathrm{Tar}}$ onto $\mathbf{C}_{\mathbf{Ref}}$ lands ($s_i = \{\boldsymbol{x}_{\mathrm{Ref}}, \boldsymbol{x}_{\mathrm{Ref+1}}\}$ in this example).

Let $\boldsymbol{x}_{\mathrm{Tar}}$ be a target ecological state in a cyclical trajectory **T**, associated with a target time t_{Tar} and a target date $đ_{\mathrm{Tar}}$, for which we want to compute a cyclical shift. Let then $\boldsymbol{x}_{\mathrm{Ref}}$ be an ecological state of reference such that $đ_{\mathrm{Ref}} = đ_{\mathrm{Tar}}$ and $t_{\mathrm{Ref}} < t_{\mathrm{Tar}}$. The ecological states $\boldsymbol{x}_{\mathrm{Tar}}$ and $\boldsymbol{x}_{\mathrm{Ref}}$ can be respectively associated with unique cycles $\mathbf{C}_{\mathbf{Tar}}$ and $\mathbf{C}_{\mathbf{Ref}}$ starting half a cycle duration ($\mathrm{DUR}_{\mathrm{C}}/2$) before t_{Tar} or t_{Ref} and ending half a cycle duration after. In other words, the target and reference ecological states lie in the middle of those cycles (Figure 3). Let now s_i be the directed segment of $\mathbf{C}_{\mathbf{Ref}}$ onto which the orthogonal projection of $\boldsymbol{x}_{\mathrm{Tar}}$ falls (Figure 3, note that s_i can be any segment of $\mathbf{C}_{\mathbf{Ref}}$ independently of the associated dates). Then $t_{\mathrm{Proj}} = t_i + (t_{i+1} - t_i) \times \mathrm{R}(\boldsymbol{x}_{\mathrm{Tar}}, s_i)$ will be the time corresponding to the orthogonal projection of $\boldsymbol{x}_{\mathrm{Tar}}$ onto $\mathbf{C}_{\mathbf{Ref}}$. From there, the cyclical shift Δ_t can be computed in time unit as

$$\Delta_t = t_{\mathrm{Proj}} - t_{\mathrm{Ref}}. \tag{4}$$

The corresponding cyclical shift in relative position can be computed as $\Delta_R = R(\boldsymbol{x}_{\mathrm{Tar}}, \mathbf{C}_{\mathbf{Ref}}) - R(\boldsymbol{x}_{\mathrm{Ref}}, \mathbf{C}_{\mathbf{Ref}})$ (Figure 3).

Negative values of Δ_t (or Δ_R) indicate that the target ecological state $\boldsymbol{x}_{\text{Tar}}$ is less far along $\mathbf{C}_{\mathbf{Ref}}$ than the reference ecological state $\boldsymbol{x}_{\text{Ref}}$ (i.e., an ecological state less "advanced" at the same date) and is interpreted as a delay. Conversely, a positive value of Δ_t indicate that $\boldsymbol{x}_{\text{Tar}}$ is further away along $\mathbf{C}_{\mathbf{Ref}}$ than $\boldsymbol{x}_{\text{Ref}}$ (i.e., an ecological state more "advanced" at the same date) and is interpreted as an advance. Note that the sign associated with advances or delays is opposite to the dominant convention in phenology where advances are associated with negative numbers, whereas delays are associated with positive numbers (see examples in Schwartz, 2013). This difference arises because phenology most often compares the different timings of the same ecological event (i.e., time is the variable to explain) whereas here, we compare different ecological states occurring on the same date (i.e., time is a given).

In most cases, we argue that it would be desirable to center $\mathbf{C}_{\mathbf{Tar}}$ and $\mathbf{C}_{\mathbf{Ref}}$ (with respect to their internal ecological states) before estimating cyclical shift. This is because the notion of cyclical shift is concerned with the date of a cycle a particular ecological state is reached. This requires those two cycles to be somewhat comparable (i.e., going through roughly the same ecological states) and centering improves this comparability. Even after centering, it should be stressed that it may have little sense to compute cyclical shifts for cycles that are very dissimilar (both in terms of shape and position), and we expect the degree of tolerable dissimilarity to change in a case-by-case manner as a function of peculiar applications. Nonetheless, tests of cyclical shift robustness using artificial data manipulating noise and shape differences between $\mathbf{C}_{\mathbf{Tar}}$ and $\mathbf{C}_{\mathbf{Ref}}$ suggest that cyclical shifts measures behave generally satisfactorily (Appendix S2). Critically, cyclical shifts are not biased by noise towards either delays or advances.

Summary of the CETA framework

CETA allows to rigorously split cyclical trajectories into cycles $\mathbf{C}$ and fixed-date trajectories **fdT** (Figure 4a–c) and compute the metrics describing their geometries. The Ω_{C} and Ω_{fdT} spaces associated to cycles and fixed-date trajectories respectively (Figure 4d,e) allow to isolate and study different aspects of cyclical trajectories (change in cycle characteristics, similarity in long-term dynamics along cycles revealed by fixed-date trajectories). Finally, CETA generalizes the phenological notion of advance and delays to the multidimensional case by allowing computing cyclical shifts.

Functions allowing to define and analyze the trajectories studied by CETA are available along with functions for classical ETA in the "ecotraj" R package available on CRAN and GitHub repositories (https://emf-creaf.github.io/ecotraj/).

ECOLOGICAL APPLICATIONS

Seasonal dynamics in a shorebird community

The arrival and departure of shorebirds from given sites along their migratory flyways results in strong seasonal patterns in local bird communities. Given that over half of shorebird populations, particularly migrating ones, are currently decreasing in response to global changes (BirdLife International, 2021), it is likely that local seasonality in bird communities is changing. Yet, changes in seasonality in birds are mostly considered at the population level using unidimensional metrics of phenology. A community-level analysis of seasonality, such as proposed by CETA, would be complementary to existing approaches and would enhance our view of shorebirds as bioindicators (Durant et al., 2009; Piersma & Lindström, 2004) or as factors of ecosystemic changes (van der Meer et al., 2001).

Ecological context and data source

The Bay of Saint-Brieuc (Brittany, France) is a temperate tidal bay in the southern part of the English Channel. It includes about 29 km^2 of tidal flats in its southern part that serve as a wintering site for shorebirds (between 10,000 and 15,000 individuals in total during winter months; Sturbois & Ponsero, 2019; Sturbois et al., 2024). The Réserve Naturelle de la Baie de Saint-Brieuc, covering 11.4 km^2 of the tidal flats, was created in 1998 to protect the shorebirds and supports regular monitoring of their populations, following long-term trends and assessing ecological quality of marine habitats (Durant et al., 2009; Piersma & Lindström, 2004). We use a monthly resolved subset of the counts performed by the managers of the natural reserve of the Bay of Saint-Brieuc between 2001 and 2023 for 18 shorebird species (Sturbois et al., 2024; Sturbois & Ponsero, 2019).

Application of CETA and discussion

The raw shorebird count data were first expressed as percentage difference (*alias* Bray–Curtis distance; Bray & Curtis, 1957; Odum, 1950) to define the Ω_0 space. Because the shorebird populations are wintering in the Bay, seasonal cycles were defined from June to June,

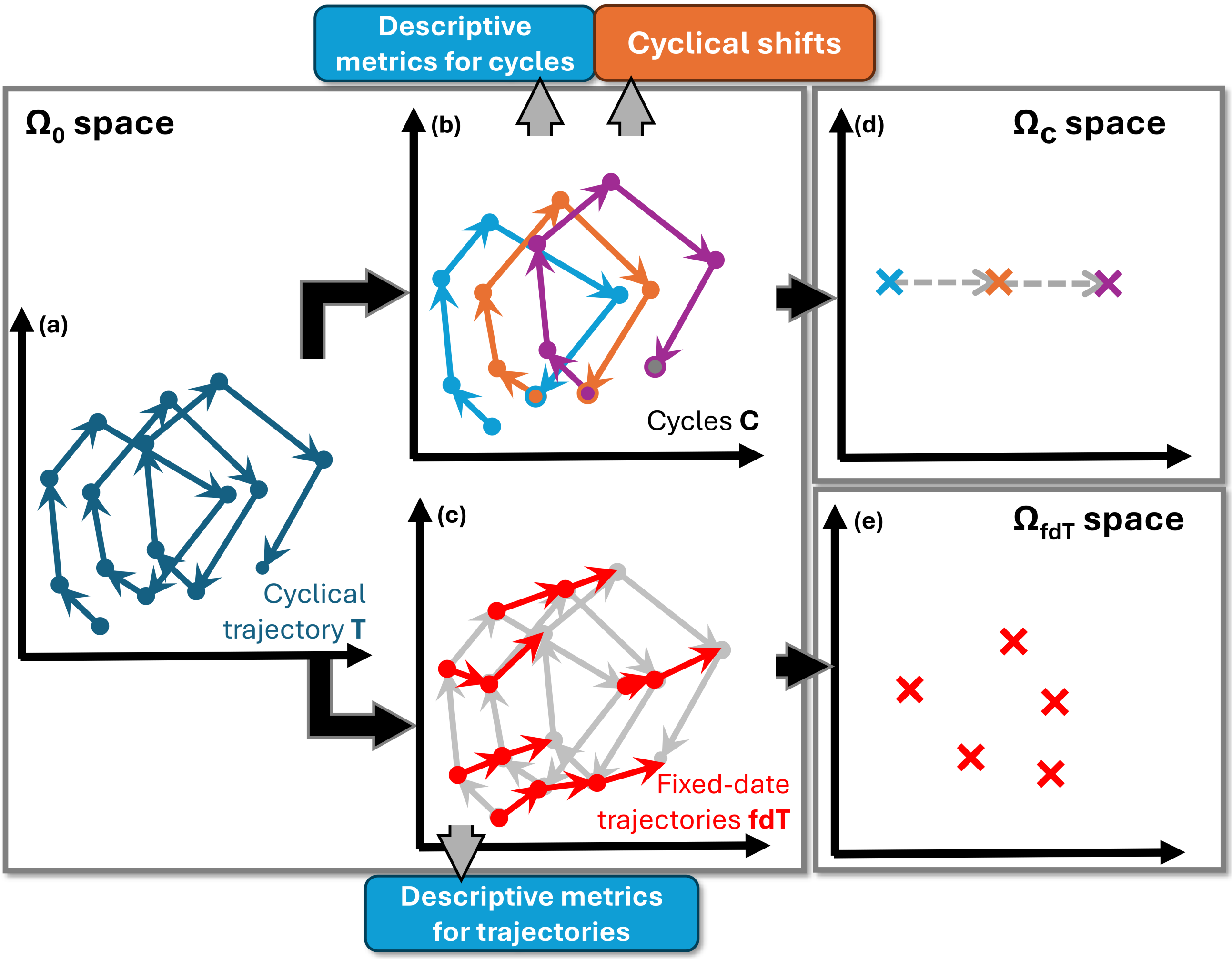

FIGURE 4 Graphical summary of the Cyclical Ecological Trajectory Analysis (CETA) framework: In the Ω_0 space, from the original cyclical trajectory (a), it is possible to distinguish cycles, as special case of trajectory sections (b), and fixed-date trajectories (c). Each can be described using a suite of metrics. CETA opens the possibility to work on the spaces defined by the resemblance between cycles or fixed-date trajectories allowing to focus on cyclical dynamics (Ω_C space, d) or on trends for each date along cycles (Ω_{fdT} space, e). Note that because cycles will be time-ordered in most applications, the Ω_C space can serve as the basis for second-stage trajectory analysis (gray dotted arrows in d).

when population abundances are minimal. Visualization of the cycles in the Ω_0 space (Figure 5a) reveals a clear seasonal pattern (summer communities towards the left of the ordination, winter communities towards the right). A closer inspection suggests a long-term change in cycle shapes and positions with a downward movement along PCoA axis 2 in time. (Figure 5a). This is confirmed by an ordination on the distances between cycles (i.e., inspection of the Ω_C space obtained using D_{SDSP} as a pairwise trajectory dissimilarity measure; De Cáceres et al., 2019) where long-term change is evident along PCoA axis 1 (Figure 5b). This temporal trend was found to be statistically significant (Mann–Kendall test *p*-value <0.01, Figure 6a) and can be linked with some readily identified long-term changes in some of the dominant species of the community (i.e., decrease in Brants *Branta bernicla*, and increase in Sanderlings *Calidris alba* and Eurasian curlews *Numenius arquata*, data not shown, see Sturbois et al., 2024).

Another aspect of changing seasonality in the shorebird community of the Bay of Saint-Brieuc is revealed by the increasing trend in cycle convexity and decreasing trend in cycle length (Figure 7b,c, both significant, Mann–Kendall test *p*-value <0.01). An interpretation is that seasonal cycles became more stable and regular (i.e., less noisy) with time. This is in agreement with the decreasing trend in LCdBD (De Cáceres et al., 2019; Legendre & De Cáceres, 2013, statistically significant, Mann–Kendall test *p*-value <0.01, Figure 6d) indicating that the most peculiar cycles with respect to the studied period are at the beginning of the series. This stabilization (reduced variability) in the seasonal

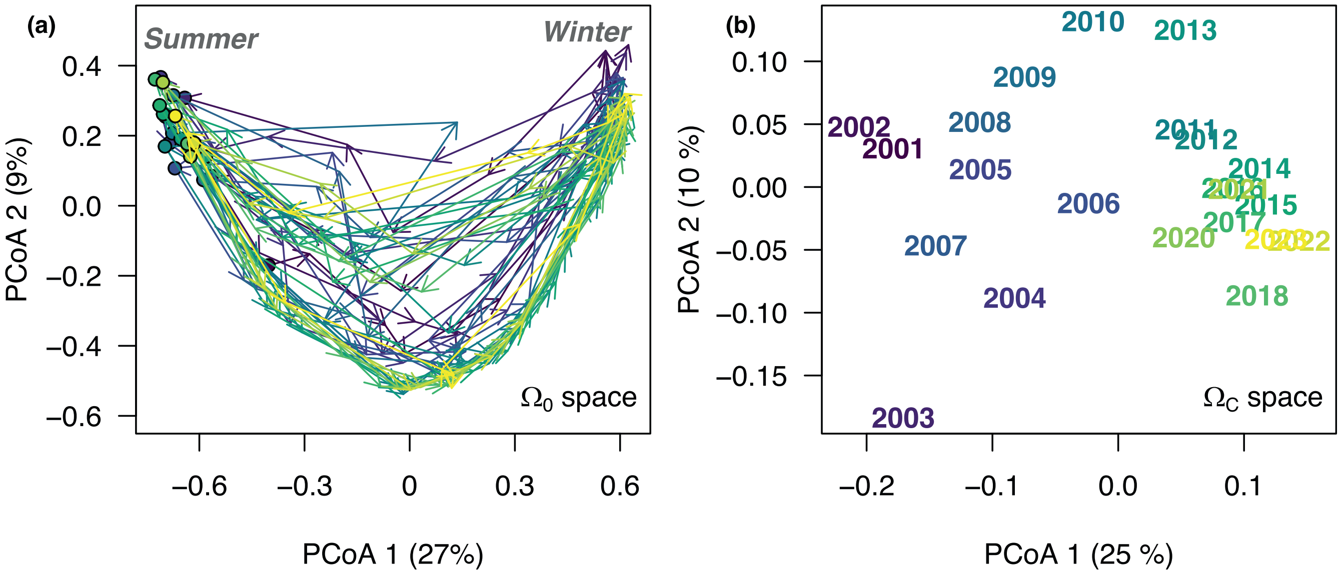

FIGURE 5 Seasonal cycles in the shorebird community of the Bay of Saint-Brieuc (a) in the Ω_0 space (based on percentage difference dissimilarity between ecological states) and in (b) the Ω_C space (based on D_{SDSP} dissimilarity between cycles). The color gradient indicates time (purple = beginning of the time series, yellow = end of the time series), solid points in (a) indicate the month of June, the start of the cycles.

cycle over 20 years is not easily seen using traditional population-level analyses and illustrates the unique insights that CETA has the potential to reveal about community-level seasonal dynamics.

Long-term changes in the seasonal dynamics of North Sea zooplankton

Marine zooplankton communities most often present strong seasonal dynamics superimposed on long-term changes (Mackas et al., 2012), making them good examples for the application of CETA. Below, we apply CETA to long-term (1958–2021) monthly resolved data on North Sea zooplankton community composition and compare our insights to what is already known of the system.

Ecological context

The North Sea is a shallow (generally <100 m deep), temperate, shelf sea of the North-East Atlantic Ocean which has experienced several abrupt changes in its ecology since 1960 widely understood as large-scale regime shifts (Beaugrand, 2004; Beaugrand et al., 2014; Weijerman et al., 2005). The North Sea regime shifts are characterized by changes in plankton biomass, population dynamics, and taxonomic and functional community composition (Beaugrand & Ibanez, 2004; Di Pane et al., 2022; Djeghri et al., 2023) with drivers ranging from large-scale climatic forcings (Beaugrand, 2004) to regional alterations of connectivity with the Atlantic (Kléparski et al., 2024) or variations in riverine nutrient inputs (Alvarez-Fernandez et al., 2012).

Of interest to the present work, the North Sea regime shifts had clear impacts on the seasonal dynamics of plankton communities. This is evident from a population-centric perspective, where many species show phenological changes in the timing of their seasonal population peak (Beaugrand & Kirby, 2018; Chivers et al., 2020; Corona et al., 2024). This is also evident at the community level, with changes in the patterns of seasonal plankton successions (Djeghri et al., 2023; Nohe et al., 2020).

Data source and preprocessing

We use here a subset of the zooplankton community composition data from the Continuous Plankton Recorder (CPR) survey (Helaouët, 2024) operated by the Marine Biological Association of the United Kingdom. The details of CPR sampling and counting procedures are given in Batten et al. (2003) and Richardson et al. (2006). Briefly, ships of opportunity (cargos, ferries…) tow CPR samplers along their commercial routes. The sampling is performed at subsurface (5–10 m depth) on a 270-μm mesh silk preserved in formalin. A typical CPR sample represents around 10 nautical miles of towing and 3 m^3 of sampled volume (Jonas et al., 2004). The CPR

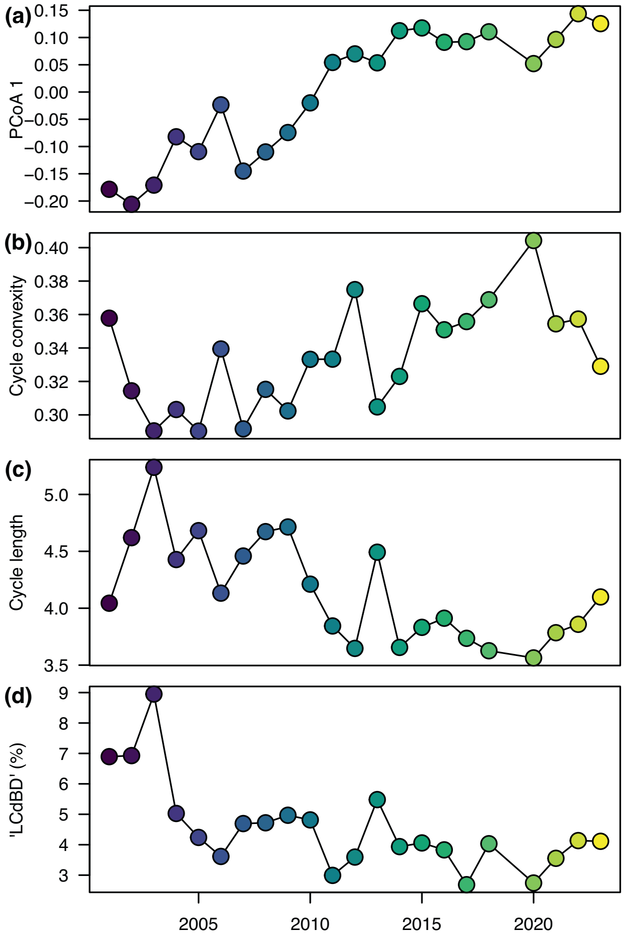

FIGURE 6 Trend in the properties of the seasonal cycles in the Bay of Saint-Brieuc's shorebird community: (a) trend along the first axis of the Ω_C space, (b) increase in cycle convexity, and (c) decrease in cycle length, (d) decrease in "Local contribution to dynamic Beta Diversity" (LCdBD) indicating that the most peculiar seasonal cycles are at the beginning of the time series. All trends are significant (Mann–Kendall tests, *p*-values <0.01).

methodology has been kept consistent since 1958, ensuring inter-comparability of samples across time.

The CPR samples of the North Sea between 1958 and 2021 were separated into two areas: the Southern North Sea (SNS, from 51 to 55° N) shallower, often tidally mixed, and under strong riverine influence; and the Northern North Sea (NNS, from 55 to 56° N), deeper, generally seasonally stratified, and under more direct Atlantic Ocean influence (Zhao et al., 2019). This broad separation helps distinguish some important ecological processes (latitudinal variation, oceanic influence vs. coastal influence) while keeping sufficient sampling to obtain almost complete, monthly resolved, time series. Because the CPR samples large areas of the North Atlantic since a long period, zooplankton taxa were screened to remove taxa not counted consistently since 1958 and remove rare taxa present in <1% of NNS and SNS samples leaving 25 taxa remaining representative of North Sea zooplankton. The abundances of the remaining zooplankton taxa were then averaged monthly to compute two time series (NNS and SNS). The time series were smoothed by averaging five data points (a 3--month moving window + the corresponding months of the previous and next year, allowing one missing value) with the aim to reduce noise, particularly in winter months due to low plankton abundances. Finally, zooplankton abundances were Hellinger-transformed. The Hellinger transformation is suitable for ecological studies (Legendre & Gallagher, 2001) and implies that only relative abundances are taken into account, complementing well previous studies on North Sea plankton mostly focused on absolute abundances (Beaugrand, 2004).

Application of CETA and discussion

We applied CETA to the two zooplankton community times series, extracting cycles for each complete year (January-to-January) and fixed-date trajectories for each month. As expected, both NNS and SNS zooplankton communities presented clear seasonal cycles in the Ω_0 space (Figure 7a). Long-term dynamics are also apparent in the Ω_0 space with cycles moving towards negative values of PCoA axis 2 and appearing to change shape (e.g., elongation along PCoA axis 1 in SNS) as time advances (Figure 7a). The change of shape in the seasonal cycles is further confirmed by studying changes in seasonal cycles length (Figure 7b) and convexity (Figure 7c). After the 1980s, cycle length decreased in SNS zooplankton communities while cycle convexity started to present an upward trend in both the NNS and SNS. This change in zooplankton's seasonal dynamics picked up by CETA is consistent with the timing of a readily identified regime shift in the North Sea ecosystem (Beaugrand, 2004; Weijerman et al., 2005). Our analysis shows that seasonal dynamics of zooplankton communities from the NNS and SNS presented parallel change over the study period (i.e., mostly parallel second-order trajectories obtained from centered cycles in the Ω_C space based on D_{SDSP}, Figure 7d), with major changes corresponding to the 1980s and the end of the 1990s, again tied to readily known regimes shifts years (Alvarez-Fernandez et al., 2012; Beaugrand, 2004; Beaugrand et al., 2014). This suggests that changing seasonality in the SNS and NNS had similar drivers (presumably mostly climatic as suggested in previous works; Kléparski et al., 2024) but that the two region nonetheless remained dissimilar in seasonal dynamics, likely due to the latitudinal gradient and their different hydrodynamic characteristics (Zhao et al., 2019).

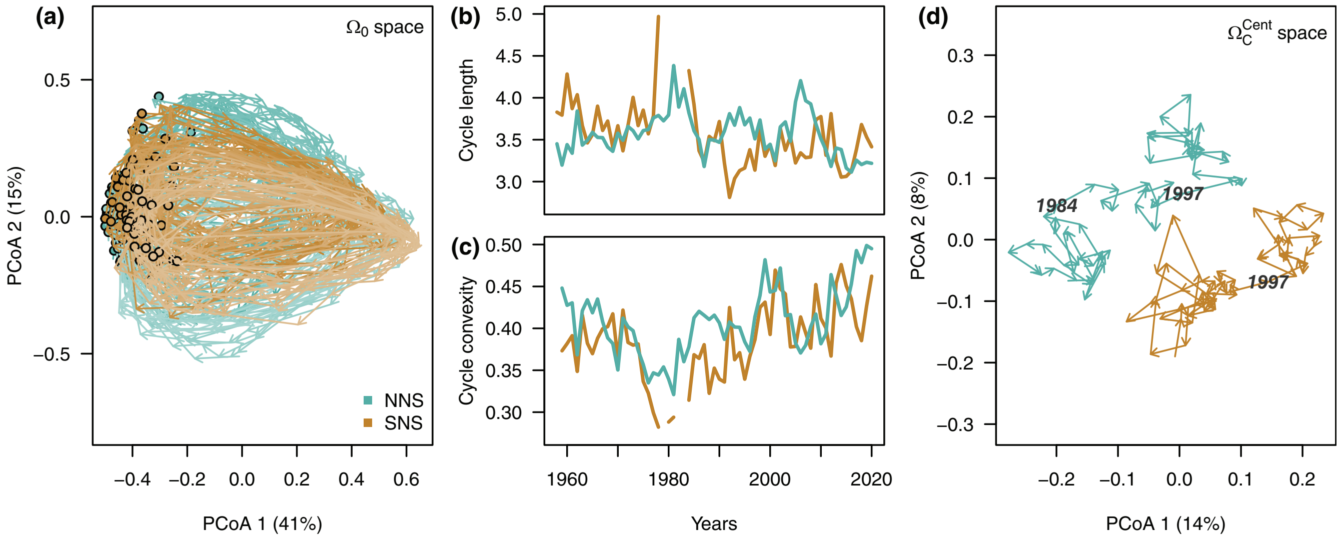

FIGURE 7 Long-term change in the zooplankton community composition seasonal cycles in Northern North Sea (NNS) Southern North Sea (SNS). (a) Seasonal cycles in the Ω_0 space, lighter colors indicate more recent years, solid points correspond to the month of January (start of cycles). Time series of cycle length (b) and convexity (c). Second-stage trajectories in the Ω_C space obtained from centered cycles (d), each point linked by arrows represents one seasonal cycle, years of important change are indicated in gray (see text).

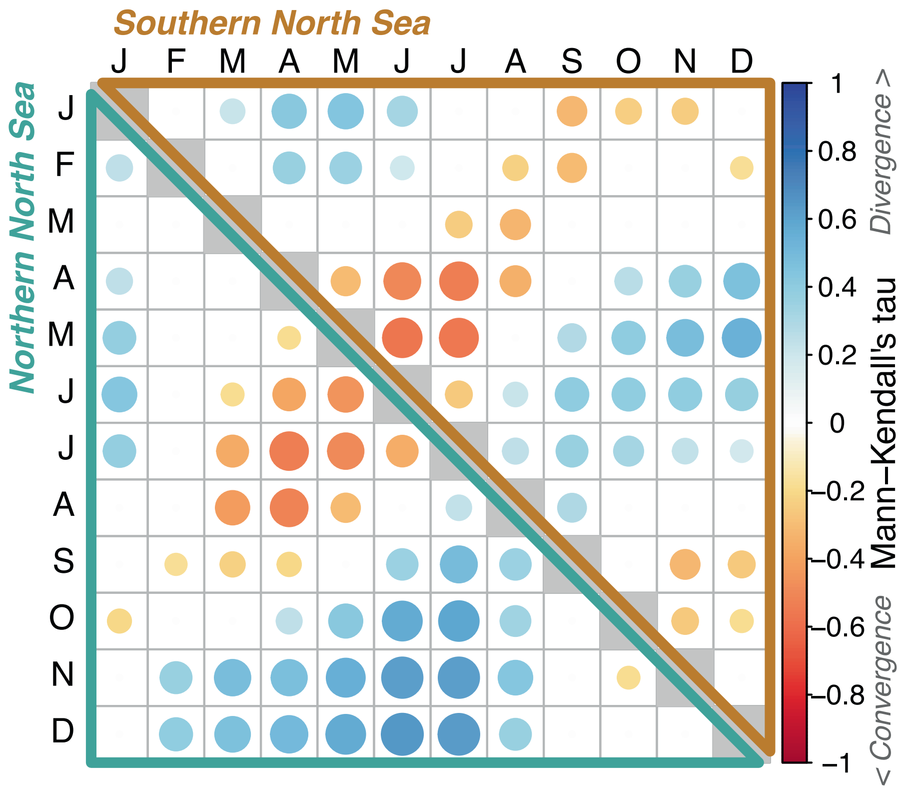

FIGURE 8 Convergence (red) or divergence (blue) between fixed-date trajectories (i.e., trajectories associated to each month) in the Northern North Sea (lower triangle) and Southern North Sea (upper triangle) zooplankton communities. The Mann–Kendall tau statistic is represented by the size and color of the circles. Only significant (alpha <0.05) trends are indicated.

Studying fixed-date trajectories allows to further specify the change in seasonality in the SNS and NNS zooplankton communities. Figure 8 presents result from symmetric convergence tests between fixed-date trajectories (Mann–Kendall test; De Cáceres et al., 2019). In both the SNS and NNS, the same broad patterns emerge: Over

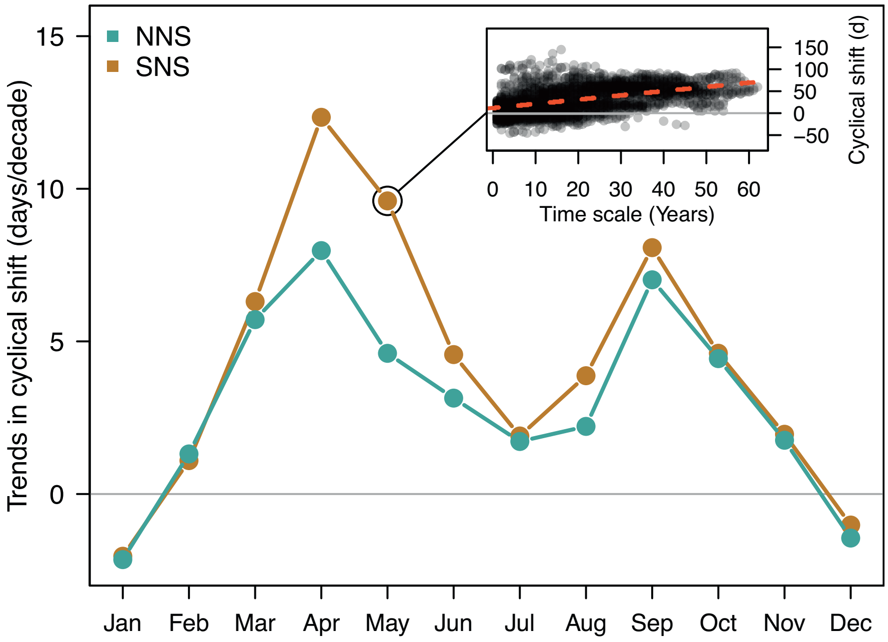

FIGURE 9 Trends in community-level cyclical shifts in the Northern North Sea (NNS) and Southern North Sea (SNS) zooplankton. The insert graph shows an example of the computation of the trend for the month of May in the SNS (i.e. the black points are cyclical shifts measured using Cyclical Ecological Trajectory Analysis (CETA), the trend in cyclical shift corresponds to the slope of the orange dotted line).

the years, zooplankton communities observed during spring bloom months (April, March) converged with summer months communities (June, July, August). Simultaneously, the zooplankton community composition of spring and summer months diverged from that of winter months (November, December, and to a lesser extent, October and January). This suggests that spring and summer zooplankton composition became more homogeneous, indicating reduced seasonal differentiation during those months in recent years, while the contrast between winter and summer increased.

Finally, CETA allows computing cyclical shifts for multidimensional data (e.g., measures of “phenological” advance and delays at the community level). For this example, we computed all possible cyclical shifts for each month in the NNS and SNS zooplankton communities (e.g., amounting to 2016 cyclical shift computed for each month in the complete NNS time series, resulting from all possible combinations of target and reference cycles). Taking inspiration from the study of spatial species turnover (Graco-Roza et al., 2022), we derive a robust and synthetic measure of temporal shift across the entire time series from the relationship between the observed cyclical shifts and their corresponding time scales (i.e., time elapsed between the target and reference cycles, see insert in Figure 9). The slopes of the cyclical shift-time scale relationship represent an estimate of the rate of cyclical shift (expressed in days of advance or delay per decade). This procedure has the advantage of using all potential combinations of target and reference cycles, avoiding an arbitrary choice of reference, and limiting the impact of the rather high variability at interannual scale (see dispersion in the insert in Figure 9). We find that cyclical shifts in the North Sea zooplankton communities are positive overall (except in December and January, Figure 9), indicating an advance in community composition. The advance presents strong seasonal patterns coherent between the NNS and the SNS with maximums in April and September, corresponding to the transition periods between summer and winter where plankton typically blooms (respectively primary spring bloom and secondary autumn bloom). The advance measured during those periods is more than 5 days per decade and indicates that the spring and autumn zooplankton communities move faster towards, respectively, summer-like and winter-like states. Note that the most prominent peak in advance reaches roughly 12 days per decade in April in the SNS. With a >60 year long time series, this implies that zooplankton community composition observed in April in the 2020s is most similar to what was typically seen in June in the 1960s. Other studies on zooplankton phenology in the region have employed population-centric methodologies on generally shorter time series and conclude that zooplankton phenology either advances (Corona et al., 2024) or do not present phenological shifts (Jan et al., 2024) These discrepancies are likely imputable to variation in the location studied (Uriarte et al., 2021) and in time series length. Although taxa-dependent, CPR phytoplankton phenological advances for individual taxa are found to be of the same order as what we find here for zooplankton (Chivers et al., 2020). The community-level seasonal advance found here is large, but not incompatible with what is known from populations, stressing how much North Sea's seasonality changed in the last few decades.

Diel activity patterns in insects with an experimental trapping system

Although we envision most applications for CETA to be linked with seasonality and observational data, the method is applicable in other settings (i.e., other types of cycles, experimental setups). Here, we present an example application of CETA to diel activity patterns of insects in an experimental context.

Ecological context

Insects are regarded as key actors of (agro)ecosystem functioning, holding important roles in carbon cycling and pollination (Elizalde et al., 2020; Médiène et al., 2011). Moreover, their roles are critically influenced by the strong diel activity patterns of their populations and communities (Cox & Gaston, 2024; Wong & Didham, 2024). However, insects' diel cycles remain understudied due to the high effort associated with sampling at sufficient rates. A way forward is the development of high-frequency smart traps that increase our capacity to resolve fine scale insect dynamics at low cost and time investment (Geissmann et al., 2022). As for any sampling device, smart traps need to be designed appropriately to answer a given scientific question, and it is necessary to assess how smart trap design may influence the pattern of diel insect activity detected. Here, we use CETA to assess the effect of presence or absence of bait on the diel activity pattern detected by an experimental smart trap: the Sticky Pi (Geissmann et al., 2022).

Data source, sampling, and preprocessing

The Sticky Pi is an insect trap that proceeds by capturing insects on a sticky plate that is regularly photographed. An image processing algorithm then detects captured insects, associates them with a capture time, and classifies them (down to family level) with the help of a convolutional neural network. Ten Sticky Pi were deployed in a blackberry field in Agassiz (British Columbia, Canada) for 7 weeks (12 August 2020–30 September 2020). Half of the traps were baited with apple cider vinegar.

The traps yielded sparse time series of insect capture times. In their original form, these data represent highly noisy trajectories not usable directly by CETA. The data were thus aggregated to obtain viable community-like averages. We averaged the data yielded by all traps under the same treatment for each hour and then over three broad periods based on trends in dominant taxa during the experiment (see fig. 5 in Geissmann et al., 2022): 12 August 2020–5 September 2020, 6 September 2020–24 September 2020, and 25 September 2020–30 September 2020, allowing us to reconstruct average diel cycles for the three periods. The following analysis is therefore based on six cycles (3 periods × 2 treatments), each constituted of 24 ecological states (one per hour of the day).

Application of CETA and discussion

The Ω_0 space was computed from percentage difference dissimilarities. Fixed-date trajectories (joining the same hours across the different cycles) were extracted (Figure 10a,b) and centered (defining the Ω_0^{Cent} space, Figure 10c,d) to assess differences between fixed-date trajectories independently of average community composition (i.e., trajectory position). Visualization of the Ω_0^{Cent} space showed that broadly defined night (from 19:00 to 5:00) and day (from 5:00 to 19:00) centered fixed-date trajectories generally pointed in different directions (Figure 10c,d), suggesting different community dynamics between day and night irrespective of average differences in communities.

To test the effect of day and night and the effect of the bait, we computed dissimilarities between fixed-date trajectories (D_{SDSP}) and represented them in the Ω_{fdT} space (Figure 11). Non-centered fixed-date trajectories from day and night and baited and control treatments generally grouped in distinct clusters (Figure 11a). After testing for heterogeneity of variances between groups (nonsignificant at alpha $= 0.05$), we tested the effect of night and day and bait on the non-centered fixed-date trajectories through permutational multivariate analysis of variance (PERMANOVA; Anderson, 2001) and found a significant effect of both factors and their interaction (p-values <0.05). In contrast, centered fixed-date trajectories appeared little distinguished by presence or absence of bait (Figure 11b, although the distinction between night and day remains clear along PCoA axis 1 representing 57% of variance). The variances of the groups were found to be heterogeneous precluding the application of PERMANOVA for formal testing. Nonetheless, our results suggest that first, insect activity patterns of night and day experienced different dynamics through the experiment (night and day fixed-date trajectories remained different after

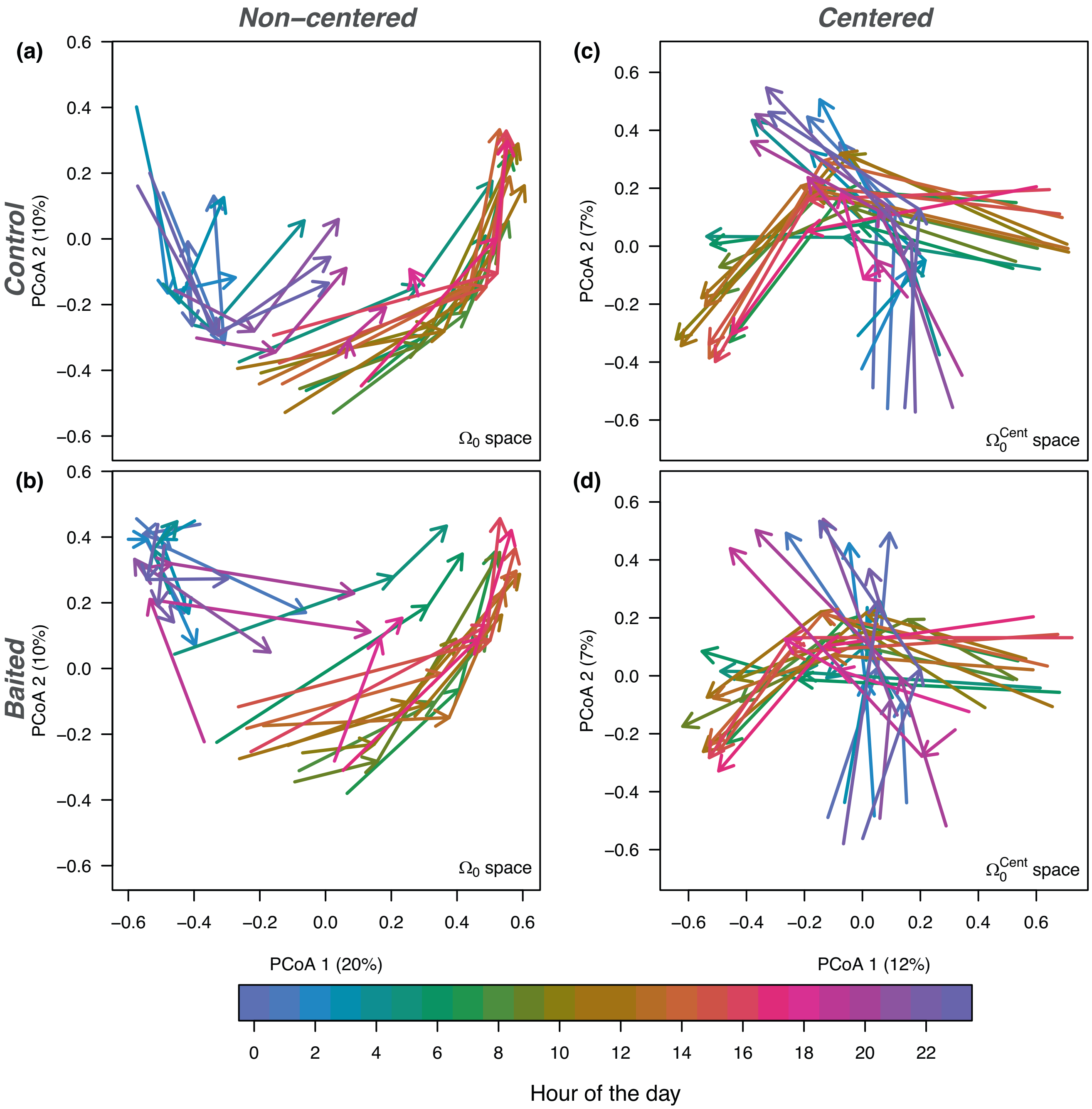

FIGURE 10 Fixed-date trajectories in the Ω_0 space before (a, b), and after centering (c, d) representing insect daily activity patterns as captured by Sticky Pi traps. The upper panels (a, c) present fixed-date trajectories in the control Sticky Pi traps (i.e., without bait) and the lower panels (b, d) present fixed-date trajectories in the baited Sticky Pi traps. Although presented on different panels, control and baited treatment are analyzed in the same ordination.

centering). Second, our results suggest that baiting resulted in different trajectories in terms of positions (different non-centered fixed-date trajectories, Figure 11a) linked to the attraction of some specific taxa (in this case, Drosophilidae, see detailed results in Geissmann et al., 2022). However, the treatment (i.e., presence/absence of bait or indirect effects of the presence of more Drosophilidae) had a limited impact on the dynamics of the other taxa (similar baited and controlled centered fixed-date trajectories, Figure 11b).

Deciphering intertwined cyclical dynamics: High-frequency environmental data in a system under diel, tidal, and seasonal forcings

Time series, particularly if sampled at high frequency, may contain several embedded cyclical dynamics (Fulton et al., 2019). In this example, we use high-frequency marine environmental data with complex temporal

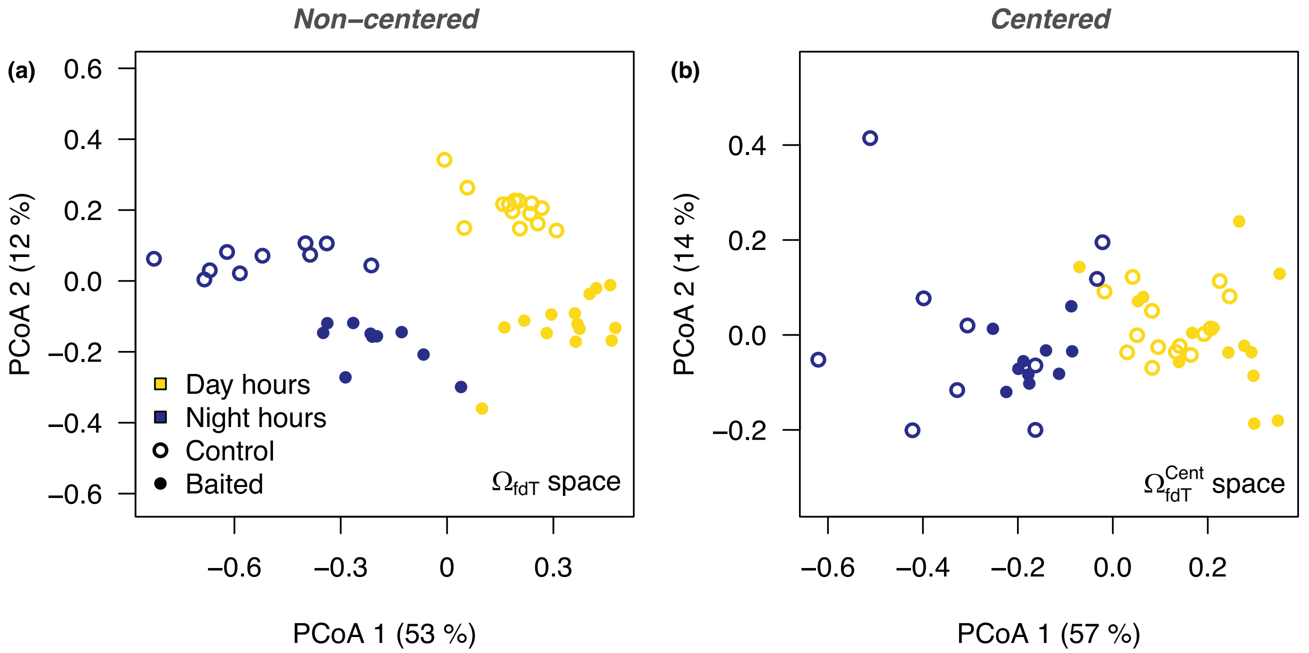

FIGURE 11 Dissimilarities between fixed-date trajectories (D_{SDSP}) obtained from insects' daily activity patterns before (a) and after (b) centering.

dynamics (seasonal trend, diel, and tidal cycles) to illustrate how CETA can be articulated with multiscale analysis to isolate and describe cyclical dynamics of interest.

Ecological context

The Bay of Brest (Brittany, France) is an enclosed, 180 km^2, temperate marine system marked by important tides with an exchange volume reaching 40% of high tides volumes during the spring tides (Poppeschi et al., 2022). The macrotidal nature of the system has a deep impact on its ecology, protecting somewhat the Bay from eutrophication (Ragueneau et al., 2018) and controlling the seasonal dynamics of the phytoplankton communities (Quéguiner & Tréguer, 1984; Ragueneau et al., 1996). At finer temporal scales (days, hours), alternance of low and high tides results in changing environmental conditions. In this context, CETA can be used to provide a description of changes in the characteristics of seawater during the tide cycle (~12.5 h).

Data source

High-frequency (~20 min) data on seawater characteristics (salinity [PSU], temperature [in degrees Celsius], oxygen [in milliliters per liter], and fluorescence [FFU, log10 + 1 transformed]) is acquired at the entry of the Bay of Brest (48°21′48 N, 4°33′33 W) by the COAST-HF Iroise instrumented buoy (https://coast-hf.fr/). We focus on data from the month of April 2023 (2103 sampling points) as it contains few gaps and presents interesting dynamics allowing us to illustrate CETA. We obtained complementary data on the timing of high and low tides in Brest from the "Service Hydrographique Océanographique de la Marine" (SHOM, https://data.shom.fr).

Isolating the tidal signal

We modeled and isolated the tidal signal using distance-based Moran Eigenvector Maps (db-MEM, Legendre & Gauthier, 2014). db-MEM generates a set of temporal eigenfunctions through a PCoA on a truncated matrix of temporal distances. The first eigenfunctions of the PCoA model long-term (large scale) signals, whereas the next eigenfunctions model short-term (small scale) signals. The eigenfunctions are then used as linear predictors of the multidimensional data in a redundancy analysis (RDA) and a forward selection procedure (Blanchet et al., 2008) can be applied to obtain a more parsimonious RDA model and avoid overfitting. Because eigenfunctions are obtained by PCoA, they are orthogonal and subsets of eigenfunctions can be used independently to model the signal at different scales. Here, the full db-MEM model after selection of significant eigenfunctions under a double-stopping criterion (alpha <0.01, increase in adjusted $R^2 > 0.0001$) reached an

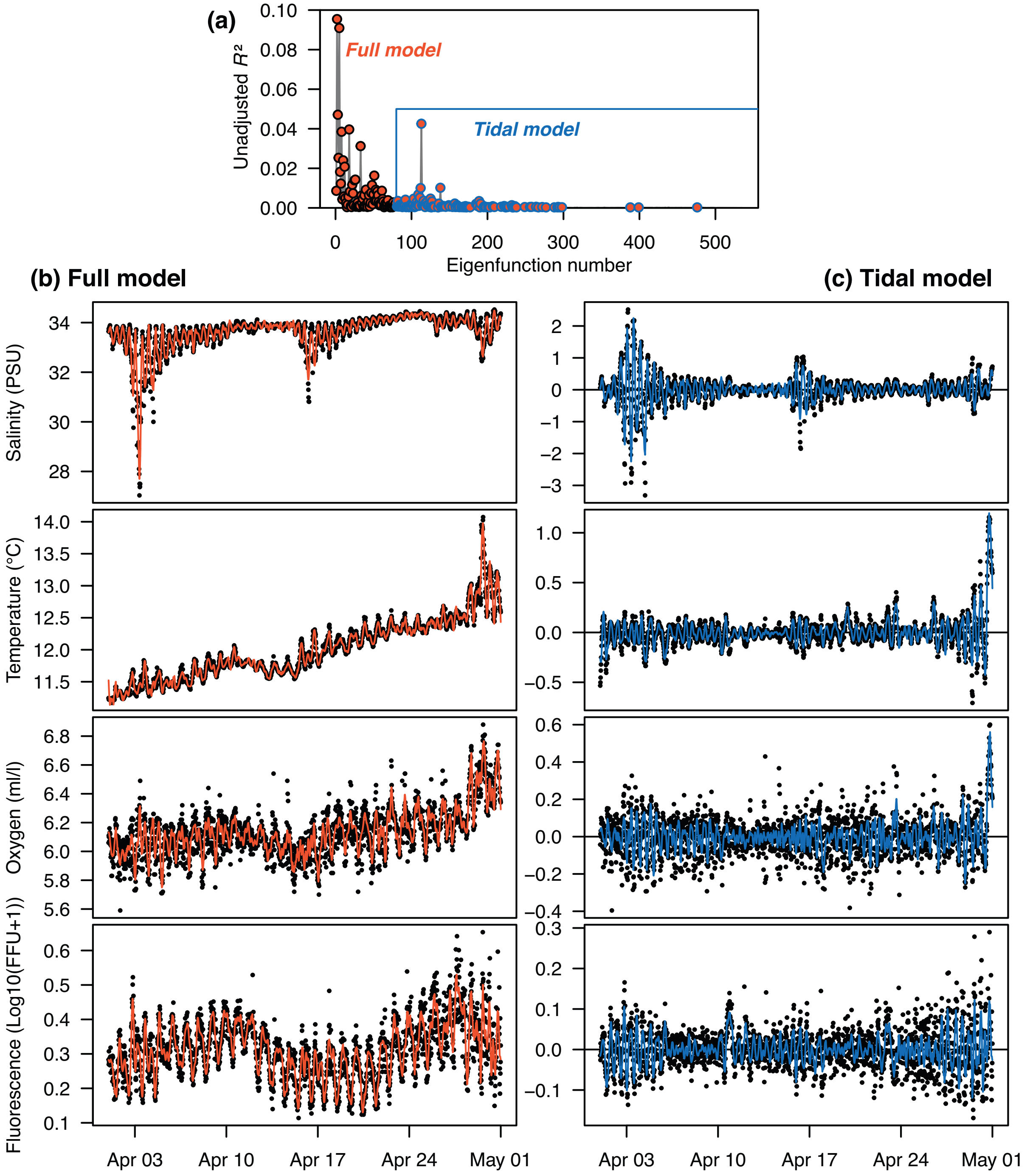

FIGURE 12 Distance-based Moran Eigenvector Maps (db-MEM) analysis of the COAST-HF data. (a) Scalogram indicating the eigenfunctions selected for the full model (orange) and for the tidal model (blue outline). (b) Full model prediction (orange) over the data (black points) and (c) tidal model prediction (blue) over the de-trended data (black points).

R^2 of 0.89 and modeled the temporal signal satisfactorily (Figure 12b). Study of the scalogram (Figure 12a) revealed that the most important eigenfunctions were among the first ones (i.e., eigenfunction 1–20) representative of large-scale signal and trends. Although not very distinct, a peak in the scalogram can be identified around eigenfunction number 50 and corresponds to a diel signal in the data (detail not shown). At smaller scales (below eigenfunction 80) the db-MEM was found to model signal at the tidal scale (Figure 12c, roughly 60 peaks are present in the modeled data corresponding to the number of tidal cycles during a month).

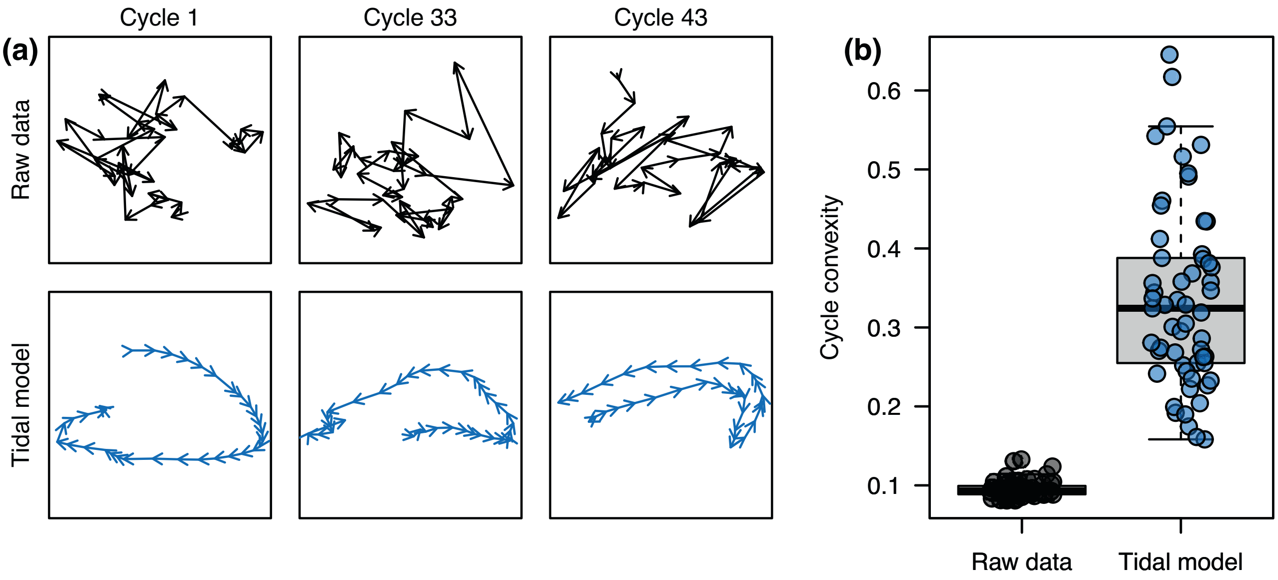

FIGURE 13 Effect of distance-based Moran Eigenvector Maps (db-MEM) modeling on (a) the shape of three randomly selected tidal cycles (visualized through principal coordinates analysis [PCoA]) and (b) on cycle convexity.

Exploring modeled data using CETA

We then apply CETA to the data modeled by the tidal model, standardizing the different variables, obtaining the Ω_0 space from Euclidean distances, and extracting tidal cycles (defined between the times of two high tides, obtained from the SHOM data). Note that because we use the output of the tidal model, the environmental data are effectively de-trended and the effect of cycles of higher amplitude (i.e., the diel cycles) on position is removed. As expected, modeling gives more regular cycles than in the raw data (Figure 13a), characterized by higher convexity (Figure 13b) denoting a drop in noise.

Further analysis of the modeled cycles revealed that their length peaked at the start, middle and end of the time series (Figure 14a), corresponding to low-salinity events (around the 3, and 16 of April), and to a high-temperature and high-oxygen event (around the 30 of April, Figure 12b,c). Studying the Ω_C space (based on D_{SDSP}, Figure 14b) shows that most tides are "typical" when controlled for the effect of trend and day-night cycles (most points are close to each other). However, some tides are "unusual" (around the 3rd, 16th, and 30th of April, Figure 14b) presenting high ecological variability within one cycle (i.e., high cycle length, Figure 14a). Our analysis further shows that the tides can be unusual in different ways denoted by their different position in the Ω_C space (towards the left are the low-salinity events, towards the bottom is the high-temperature and high-oxygen event). Note that these "unusual tides" events are at a period of roughly 14 days corresponding to the neap and spring tides cycle. In an analysis at longer time scales, these events would likely impose a secondary cyclical dynamic on the tide cycles studied here.

DISCUSSION

ETA (De Cáceres et al., 2019; Sturbois et al., 2021, 2022), in allowing to describe and compare the geometry of ecological trajectories in full multidimensional spaces, is a greatly valuable framework to study ecological dynamics (DeSiervo et al., 2023; Toumi et al., 2023; Tye et al., 2024). Yet, ETA in its previous form was not particularly fit to study cyclical dynamics that are central to many aspects of Earth's ecology (seasons, lunar cycles, days, tides...). CETA, the extension presented here, releases ETA from this limitation, pushing further its applicability, allowing it to tackle more diverse ecological questions, and opening new ways to study cyclical ecological dynamics. The major contributions of CETA are (1) its ability to rigorously subset cyclical trajectories into cycles and fixed-date trajectories that can then be described and compared using appropriate quantitative metrics and (2) its ability to compute cyclical shifts, a multidimensional equivalent of the phenological concept of advance and delays. CETA also carries over the main advantage of ETA: its grounding in dissimilarity measures, allowing working with many kinds of multidimensional ecological data without needing dimension reduction. These properties make CETA a valuable tool to dive into how ecological cyclical dynamics are structured and assess long-term changes under the

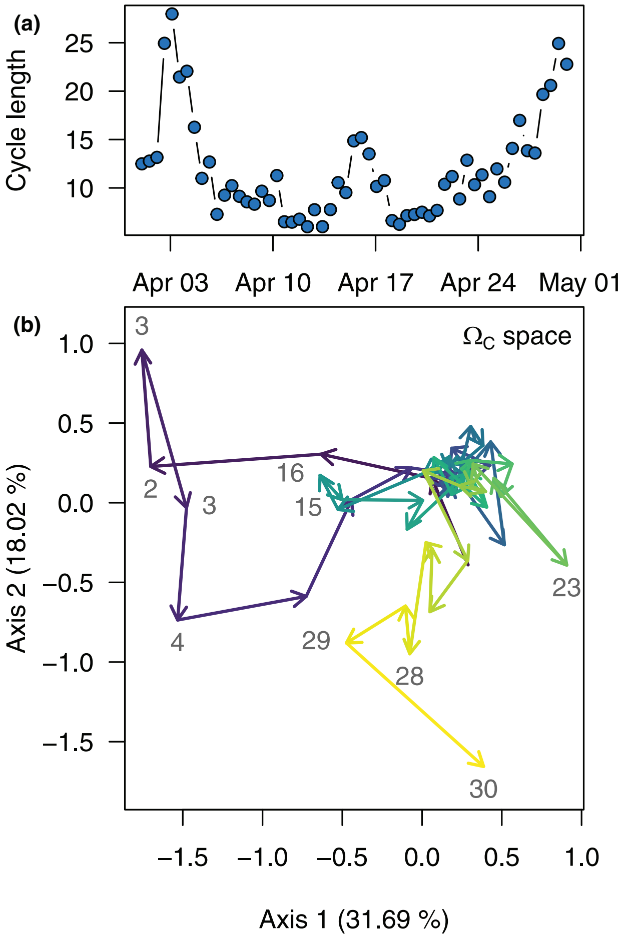

FIGURE 14 (a) Change in tidal cycle length obtained from modeled environmental data from April 2023 in the Bay of Brest (France). (b) Ordination in the Ω_C space showing dissimilarities between tidal cycles (purple: beginning of the month, yellow: end of the month, gray numbers are specific days selected to serve as reference).

influence of natural or human forcings (Behrenfeld, 2014; Cox & Gaston, 2024; Piao et al., 2019).

Use and scope of CETA

The diverse ecological examples given in this article illustrate the broad applicability of CETA, a flexibility inherited from the choice of making ETA a distance-based framework (De Cáceres et al., 2019; Sturbois et al., 2022). CETA is able to tackle different ecological cycles (seasons, days, tides), using different data (community composition, environmental data), in different contexts and for different purposes (observational vs. experimental). The last example on tidal cycles in the Bay of Brest also critically illustrates how CETA can be combined with multiscale analysis (Legendre & Gauthier, 2014) to describe and understand complex, intertwined multidimensional temporal dynamics. In addition to its wide applicability, CETA allows us to uncover the characteristics and the variability of cyclical ecological dynamics in multidimensional data, filling a critical gap in the ecologist's toolbox (Inouye et al., 2019). This is perhaps best illustrated by our North Sea zooplankton example showing how a phenological question of advance and delay, usually tested on unidimensional data, can now be applied to multidimensional data.

This ability of CETA to answer phenological questions using multidimensional data makes it a promising tool to strengthen the links between phenology and community ecology (Inouye et al., 2019). We suggest that this link could be pushed further by applying CETA to matrices describing a "phenological community" (Post, 2019). In a phenological community, the traditionally used abundances are substituted by duration and/or timing of given phenophases (i.e., distinct, annually repeating, phases of organisms life cycles such as flowering, nesting etc.), driving attention towards dominance in time rather than dominance in terms of abundance. The concept of phenological communities, and potential declination at other timescales (e.g., repartition of activities in days), is particularly valuable to answer questions such as changes of temporal niches (Harrington et al., 2009; Post et al., 2016). Similarly to what is proposed by Post (2019), species abundances in the matrices used in CETA may be replaced by numbers or proportions of individuals engaged in a specific phenophase. In this case, CETA would allow to describe variation in the cyclical activities of organisms rather than cyclical variation in abundances.

It is worth noting that some particularly promising applications for CETA are not illustrated in this article. A notable one is the application of CETA in trait-based ecology, a rapidly growing sub-field of ecology (Palacio et al., 2022). Trait-based ecology has methods to transform compositional spaces (such as the ones illustrated here) into functional spaces using species- or individual-level trait data (Carmona et al., 2016; Mammola et al., 2021; Villéger et al., 2008). Hypotheses on ecosystem functioning can then be tested by linking traits to specific responses or effects on the environment (Suding et al., 2008). In this context, the CETA framework will facilitate testing hypotheses about cyclical dynamics in functional spaces.

Another potential application of CETA, and perhaps of ETA more generally, lies in studying the coupling of phenomena occurring at different temporal scales. For example, envision a long-lived predator population, varying predominantly at interannual scale, monitored once a year. This predator population is feeding on a seasonally varying prey community monitored monthly. CETA allows to build a one-for-one correspondence between the two datasets by extracting annual cycles from the prey community time series. Although this can be done with other methods (e.g., averaging), CETA metrics preserve much more information on cycles characteristics, particularly when using dissimilarities between cycles in the Ω_C space. Hence, coupling between a cyclical phenomenon and larger scale drivers or responses may be studied using CETA. We suggest that this can be achieved by relating dissimilarities between cycles (the Ω_C space) to larger scale variables using distance-based redundancy analysis (db-RDA; Legendre & Anderson, 1999; McArdle & Anderson, 2001).

Finally, we suggest that CETA may find valuable application outside of ecology, in fields interested in cyclical dynamics such as chronobiology, which often deals with multidimensional physiological, behavioral, or omics data (Hurley et al., 2018; Thornton et al., 2024).

CETA and other components of the ETA framework

As an extension of ETA, CETA is readily compatible with two adjacent frameworks: Ecological Quality Assessment (EQA; Sturbois et al., 2023) and Ecological Dynamic Regimes (EDRs; Sánchez-Pinillos et al., 2023). The combination of CETA with EQA and EDR opens promising research avenues:

EQA (Sturbois et al., 2023) is a tool for ecosystem management where reference envelopes—considered "good" ecological status—can be defined from either ecological states (a static reference) or trajectories (a dynamic reference). Combining CETA and EQA would allow to define cyclical dynamics as reference and assess whether a cycle of interest lies within or outside typical cycles. This could greatly help management of ecosystems or communities that are inherently cyclic. One example is seasonally varying plankton communities for which assessment frameworks taking seasonality into account are needed (Tett et al., 2008).

EDR (Sánchez-Pinillos et al., 2023) is a framework to define and characterize "EDRs" as an ensemble of similar trajectories representing similar ecological dynamics (for instance trajectories of recovery after disturbances). The EDR framework includes procedures to cluster trajectories into EDRs and describe the diversity of trajectories within an EDR. Further, the framework allows comparing EDRs. Applying the EDR framework on cycles obtained by CETA would allow identifying and describing different "cyclical regimes" (e.g., seasonal regimes, or diel regimes). We suggest that if the cycles are obtained from a common time series, as we anticipate will often be the case, it might be valuable to add a time contiguity constraint (Guénard & Legendre, 2022) on the clustering approaches of the EDR framework. Broadly, uniting CETA and the EDR framework would allow assessing when cyclical dynamics shift from one regime to another and help identify potential drivers.

Caveats and recommendations regarding CETA

Before applying CETA to their own research, users should be aware of its specificities, assumptions, and limitations, and how to mitigate them. First, as for any dissimilarity-based framework, the results yielded by CETA will be highly dependent on the choice of dissimilarity coefficient. Different coefficients have different properties and emphasize different aspects of ecological entities (e.g., here we used three different coefficients as a function of data type and targeted representation of ecological communities). We refer the reader to the literature describing the properties of different dissimilarity coefficients (Legendre & De Cáceres, 2013; Legendre & Gallagher, 2001; Mammola et al., 2021; Ricotta, 2021; Tuomisto, 2010) to make an appropriate choice for a given scientific question and data type.

Second, CETA is a primarily descriptive framework allowing characterizing cyclical dynamics in multidimensional ecological datasets. CETA effectively assumes that a cyclical pattern of a user-defined frequency is present in the provided data without testing whether cycles are effectively present. If the data provided are non-cyclical or if cycles are hidden under a lot of sampling noise or natural variability, the method may yield nonsensical results. CETA users should therefore ensure that a cyclical pattern of interest is indeed present in their data before applying the method. This may be achieved visually using ordinations, or more formally using statistical methods allowing to detect and/or extract cycles in multidimensional data (see ecological example on tidal cycles). More generally, users should keep in mind that all CETA metrics will be sensitive to noise. In this regard, metrics such as cycle length or cycle convexity should be used with care as noise bias the estimate (high noise increases length and decreases convexity, convexity might even be used as a proxy for noisy cycles, Figure 13b). This is a limitation shared with the original ETA framework where metrics such as trajectory length and directionality present the same dependencies (De Cáceres et al., 2019). The precision of cyclical shift estimation decreases with noise, but our tests show that there is no directional bias (i.e., noise does not preferentially increase or decrease cyclical shifts, Appendix S2). Several solutions exist to mitigate this problem of dependency to noise including statistical modeling (ecological example on tidal cycles) or smoothing (e.g., using moving average as in the North Sea zooplankton example). It is also generally advisable to standardize sampling effort along time series before applying CETA so that time steps and uncertainty around each ecological state are as constant as possible. Critically however, smoothing and standardization should be done carefully to preserve the cyclical variations of interest in the data and avoid averaging them out.

Another limitation of CETA, directly inherited from ETA, is the somewhat abstract nature of the trajectory spaces (Ω_T for general trajectories, Ω_C and Ω_{fdT} for trajectories specific to CETA). In these spaces, dissimilarities are under the influence of the position, shape, size, and direction of the trajectories. They can be readily interpreted as resemblance in dynamics but their finer qualification (e.g., isolating which specific aspects of environments or communities change) may be challenging. To do so, it is advisable to perform regular back and forth between the trajectory space Ω_T and the ecological states spaces Ω_0 when interpreting ecological trajectories.

Finally, it should also be kept in mind that CETA, as compared to non-cyclical ETA, has higher minimum data requirement, whereas in non-cyclical ETA a trajectory of interest may be defined with as low as three ecological states (Sturbois et al., 2021), cycles will need more sampling points to be meaningfully defined. CETA therefore relies more on sustained, long-term ecological monitoring programs (Lindenmayer et al., 2012; Magnuson, 1990). Furthermore, resolving cycles that are short relative to human work schedules (e.g., diel or tidal cycles) present an additional challenge as maintaining sustained ecological observation over the clock is not easily done with traditional methods. In this context, automated instrumentation, long available for physicochemical variables (see example on tidal cycles) and increasingly developed for biotic variables (Geissmann et al., 2022; Hartig et al., 2023; Xiao et al., 2021), provide promising avenues to acquire the necessary data.

Conclusion

In conclusion, CETA constitutes a valuable extension of the ETA framework allowing it to tackle more diverse ecological questions while inheriting its main advantages (broad applicability, unique focus on ecological dynamics rather than states, no need for dimensionality reduction). Perhaps most importantly, CETA allows approaching cyclical ecological dynamics of multidimensional data in a new way, filling a critical gap in the toolbox available to ecologists and allowing them to tackle questions regarding ecological cycles from a new perspective.

ACKNOWLEDGMENTS

We acknowledge the uncountable people and institutions that provide and maintain the long-term ecological data used in this article. We thank the successive managers, and the many volunteers of the Réserve Naturelle de la Baie de Saint-Brieuc involved in maintaining the long-term shorebird series as well as the French Ministry of the Environment for funding this monitoring. The CPR survey (https://www.cprsurvey.org), providing the North Sea zooplankton data, is maintained since the 1930s by a dedicated team performing enormous hidden work: from the deployment at sea, involving ships of opportunity, to database management, through taxonomic analysis. We want to thank them here. In situ observations for the Bay of Brest were provided by the Coast-HF Iroise buoy (DOI: https://doi.org/10.17882/74004), according to the terms of the framework agreement jointly signed by IFREMER, CNRS (INSU), and UBO (on behalf of Earth-Science-Observatory- IUEM) (n°11/2-210922). COAST-HF Iroise is part of the SNO COAST-HF and IR-ILICO observation network of French coastal ecosystems (https://ir-ilico.fr). We thank those research networks, and the people involved in their day-to-day operations. This work was supported by ISblue project, Interdisciplinary graduate school for the blue planet (ANR-17-EURE-0015) and co-funded by a grant from the French government under the program "Investissements d'Avenir" embedded in France 2030.

CONFLICT OF INTEREST STATEMENT

The authors declare no conflicts of interest.

DATA AVAILABILITY STATEMENT

Data and code (Djeghri, 2025) used to produce the analyses and figures of the ecological examples are available in Zenodo at https://doi.org/10.5281/zenodo.15498230. The software implementation of Cyclical Ecological Trajectory Analysis (CETA) metrics and concepts is available in CRAN in the "ecotraj" R package, version 1.1.0 (De Cáceres et al., 2025; https://doi.org/10.32614/CRAN.package.ecotraj).

ORCID

Nicolas Djeghri https://orcid.org/0000-0001-5740-3386
Anthony Sturbois https://orcid.org/0000-0002-9219-4468
Miquel De Cáceres https://orcid.org/0000-0001-7132-2080

REFERENCES

Åkesson, S., M. Ilieva, J. Karagicheva, E. Rakhimberdiev, B. Tomotani, and B. Helm. 2017. "Timing Avian Long-Distance Migration: From Internal Clock Mechanisms to Global Flights." *Philosophical Transactions of the Royal Society B: Biological Sciences* 372: 20160252.

Alvarez-Fernandez, S., H. Lindeboom, and E. Meesters. 2012. "Temporal Changes in Plankton of the North Sea: Community Shifts and Environmental Drivers." *Marine Ecology Progress Series* 462: 21–38.

Anderson, M. J. 2001. “A New Method for Non-Parametric Multivariate Analysis of Variance.” *Austral Ecology* 26: 32–46.

Aono, Y., and K. Kazui. 2008. “Phenological Data Series of Cherry Tree Flowering in Kyoto, Japan, and its Application to Reconstruction of Springtime Temperatures Since the 9th Century.” *International Journal of Climatology* 28: 905–914.

Batten, S. D., R. Clark, J. Flinkman, G. Hays, E. John, A. W. G. John, T. Jonas, J. A. Lindley, D. P. Stevens, and A. Walne. 2003. “CPR Sampling: The Technical Background, Materials and Methods, Consistency and Comparability.” *Progress in Oceanography* 58: 193–215.

Beaugrand, G. 2004. “The North Sea Regime Shift: Evidence, Causes, Mechanisms and Consequences.” *Progress in Oceanography* 60: 245–262.

Beaugrand, G., X. Harlay, and M. Edwards. 2014. “Detecting Plankton Shifts in the North Sea: A New Abrupt Ecosystem Shift between 1996 and 2003.” *Marine Ecology Progress Series* 502: 85–104.

Beaugrand, G., and F. Ibanez. 2004. “Monitoring Marine Plankton Ecosystems. II: Long-Term Changes in North Sea Calanoid Copepods in Relation to Hydro-Climatic Variability.” *Marine Ecology Progress Series* 284: 35–47.

Beaugrand, G., and R. R. Kirby. 2018. “How Do Marine Pelagic Species Respond to Climate Change? Theories and Observations.” *Annual Review of Marine Science* 10: 169–197.

Behrenfeld, M. J. 2014. “Climate-Mediated Dance of the Plankton.” *Nature Climate Change* 4: 880–87.

BirdLife International. 2021. *European Red List of Birds* 72. Luxembourg: Publications Office of the European Union.

Blanchet, F. G., P. Legendre, and D. Borcard. 2008. “Forward Selection of Explanatory Variables.” *Ecology* 89: 2623–32.

Bray, J. R., and J. T. Curtis. 1957. “An Ordination of the Upland Forest Communities of Southern Wisconsin.” *Ecological Monographs* 27: 325–349.

Bulla, M., T. Oudman, A. I. Bijleveld, T. Piersma, and C. P. Kyriacou. 2017. “Marine Biorhythms: Bridging Chronobiology and Ecology.” *Philosophical Transactions of the Royal Society B: Biological Sciences* 372: 20160253.

Carmona, C. P., F. de Bello, N. W. H. Mason, and J. Lepš. 2016. “Traits Without Borders: Integrating Functional Diversity across Scales.” *Trends in Ecology & Evolution* 31: 382–394.

Chivers, W. J., M. Edwards, and G. C. Hays. 2020. “Phenological Shuffling of Major Marine Phytoplankton Groups over the Last Six Decades.” *Diversity and Distributions* 26: 536–548.

Corona, S., A. G. Hirst, D. Atkinson, J. Renz, M. Boersma, and A. Atkinson. 2024. “Long-Term Shifts in Phenology, Thermal Niche, Population Size, and Their Interactions in Marine Pelagic Copepods.” *Limnology and Oceanography* 69: 482–497.

Cox, D. T. C., and K. J. Gaston. 2024. “Ecosystem Functioning across the Diel Cycle in the Anthropocene.” *Trends in Ecology & Evolution* 39: 31–40.

De Cáceres, M., L. Coll, P. Legendre, R. B. Allen, S. K. Wiser, M.-J. Fortin, R. Condit, and S. Hubbell. 2019. “Trajectory Analysis in Community Ecology.” *Ecological Monographs* 89: e01350.

De Cáceres, M., N. Djeghri, A. Sturbois, and J. la De Casa. 2025. “ecotraj: Ecological Trajectory Analysis.” CRAN. [Software]. https://doi.org/10.32614/CRAN.package.ecotraj

DeSiervo, M. H., L. L. Sullivan, L. M. Kahan, E. W. Seabloom, and L. G. Shoemaker. 2023. “Disturbance Alters Transience but Nutrients Determine Equilibria during Grassland Succession with Multiple Global Change Drivers.” *Ecology Letters* 26: 1132–44.

Di Pane, J., K. H. Wiltshire, M. McLean, M. Boersma, and C. L. Meunier. 2022. “Environmentally Induced Functional Shifts in Phytoplankton and Their Potential Consequences for Ecosystem Functioning.” *Global Change Biology* 28: 2804–19.

Djeghri, N. 2025. “NicoDjeghri/CETA-EcoEx: CETA-EcoEx First Release (v1.0.0).” Zenodo. https://doi.org/10.5281/zenodo.15498231

Djeghri, N., A. Atkinson, E. S. Fileman, R. A. Harmer, C. E. Widdicombe, A. J. McEvoy, L. Cornwell, and D. J. Mayor. 2018. “High Prey–Predator Size Ratios and Unselective Feeding in Copepods: A Seasonal Comparison of Five Species with Contrasting Feeding Modes.” *Progress in Oceanography* 165: 63–74.

Djeghri, N., A. Boyé, C. Ostle, and P. Hélaouët. 2023. “Reinterpreting Two Regime Shifts in North Sea Plankton Communities through the Lens of Functional Traits.” *Global Ecology and Biogeography* 32: 962–975.

Durant, J., D. Hjermann, M. Frederiksen, J. Charrassin, Y. Le Maho, P. Sabarros, R. Crawford, and N. Stenseth. 2009. “Pros and Cons of Using Seabirds as Ecological Indicators.” *Climate Research* 39: 115–129.

Elizalde, L., M. Arbetman, X. Arnan, P. Eggleton, I. R. Leal, M. N. Lescano, A. Saez, V. Werenkraut, and G. I. Pirk. 2020. “The Ecosystem Services Provided by Social Insects: Traits, Management Tools and Knowledge Gaps.” *Biological Reviews* 95: 1418–41.

Ferreira, A. S., A. W. Visser, B. R. MacKenzie, and M. R. Payne. 2014. “Accuracy and Precision in the Calculation of Phenology Metrics.” *Journal of Geophysical Research: Oceans* 119: 8438–53.

Fulton, E. A., J. L. Blanchard, J. Melbourne-Thomas, É. E. Plagányi, and V. J. D. Tulloch. 2019. “Where the Ecological Gaps Remain, a Modelers’ Perspective.” *Frontiers in Ecology and Evolution* 7: 424.

Gaston, K. J. 2019. “Nighttime Ecology: The ‘Nocturnal Problem’ Revisited.” *The American Naturalist* 193: 481–502.

Geissmann, Q., P. K. Abram, D. Wu, C. H. Haney, and J. Carrillo. 2022. “Sticky Pi Is a High-Frequency Smart Trap that Enables the Study of Insect Circadian Activity under Natural Conditions.” *PLoS Biology* 20: e3001689.

Ghalambor, C. K., R. B. Huey, P. R. Martin, J. J. Tewksbury, and G. Wang. 2006. “Are Mountain Passes Higher in the Tropics? Janzen’s Hypothesis Revisited.” *Integrative and Comparative Biology* 46: 5–17.

Graco-Roza, C., S. Aarnio, N. Abrego, A. T. R. Acosta, J. Alahuhta, J. Altman, C. Angiolini, et al. 2022. “Distance Decay 2.0 – A Global Synthesis of Taxonomic and Functional Turnover in Ecological Communities.” *Global Ecology and Biogeography* 31: 1399–1421.

Guénard, G., and P. Legendre. 2022. “Hierarchical Clustering with Contiguity Constraint in R.” *Journal of Statistical Software* 103: 1–26.

Harrington, L. A., A. L. Harrington, N. Yamaguchi, M. D. Thom, P. Ferreras, T. R. Windham, and D. W. Macdonald. 2009. “The Impact of Native Competitors on an Alien Invasive: Temporal Niche Shifts to Avoid Interspecific Aggression.” *Ecology* 90: 1207–16.

Hartig, F., N. Abrego, A. Bush, J. M. Chase, G. Guillera-Arroita, M. A. Leibold, O. Ovaskainen, et al. 2023. “Novel Community

Data in Ecology-Properties and Prospects." *Trends in Ecology & Evolution* 39(3): 280–293.

Helaouët, P. 2024. "CPR Data Request - Nicolas Djeghri - University of Bretagne Occidentale - 23/09/2024." (Dataset). https://doi.mba.ac.uk/data/3367/1

Helm, B., M. E. Visser, W. Schwartz, N. Kronfeld-Schor, M. Gerkema, T. Piersma, and G. Bloch. 2017. "Two Sides of a Coin: Ecological and Chronobiological Perspectives of Timing in the Wild." *Philosophical Transactions of the Royal Society B: Biological Sciences* 372: 20160246.

Hurley, J. M., M. S. Jankowski, H. D. los Santos, A. M. Crowell, S. B. Fordyce, J. D. Zucker, N. Kumar, et al. 2018. "Circadian Proteomic Analysis Uncovers Mechanisms of Post-Transcriptional Regulation in Metabolic Pathways." *Cell Systems* 7: 613–626.e5.

Inouye, B. D., J. Ehrlén, and N. Underwood. 2019. "Phenology as a Process Rather than an Event: From Individual Reaction Norms to Community Metrics." *Ecological Monographs* 89: e01352.

Jan, K. M. G., B. Serandour, J. Walve, and M. Winder. 2024. "Plankton Blooms over the Annual Cycle Shape Trophic Interactions under Climate Change." *Limnology and Oceanography Letters* 9: 209–218.

Janzen, D. H. 1967. "Why Mountain Passes Are Higher in the Tropics." *The American Naturalist* 101: 233–249.

Jonas, T. D., A. Walne, G. Beaugrand, L. Gregory, and G. C. Hays. 2004. "The Volume of Water Filtered by a Continuous Plankton Recorder Sample: The Effect of Ship Speed." *Journal of Plankton Research* 26: 1499–1506.

Kléparski, L., G. Beaugrand, C. Ostle, M. Edwards, M. D. Skogen, N. Djeghri, and H. Hátún. 2024. "Ocean Climate and Hydrodynamics Drive Decadal Shifts in Northeast Atlantic Dinoflagellates." *Global Change Biology* 30: e17163.

Kudoh, H. 2016. "Molecular Phenology in Plants: In Natura Systems Biology for the Comprehensive Understanding of Seasonal Responses under Natural Environments." *New Phytologist* 210: 399–412.

Legendre, P., and M. J. Anderson. 1999. "Distance-Based Redundancy Analysis: Testing Multispecies Responses in Multifactorial Ecological Experiments." *Ecological Monographs* 69: 1–24.

Legendre, P., and M. De Cáceres. 2013. "Beta Diversity as the Variance of Community Data: Dissimilarity Coefficients and Partitioning." *Ecology Letters* 16: 951–963.

Legendre, P., and E. D. Gallagher. 2001. "Ecologically Meaningful Transformations for Ordination of Species Data." *Oecologia* 129: 271–280.

Legendre, P., and O. Gauthier. 2014. "Statistical Methods for Temporal and Space–Time Analysis of Community Composition Data." *Proceedings of the Royal Society B: Biological Sciences* 281: 20132728.

Lindenmayer, D. B., G. E. Likens, A. Andersen, D. Bowman, C. M. Bull, E. Burns, C. R. Dickman, et al. 2012. "Value of Long-Term Ecological Studies." *Austral Ecology* 37: 745–757.

Mackas, D. L., W. Greve, M. Edwards, S. Chiba, K. Tadokoro, D. Eloire, M. G. Mazzocchi, et al. 2012. "Changing Zooplankton Seasonality in a Changing Ocean: Comparing Time Series of Zooplankton Phenology." *Progress in Oceanography* 97–100: 31–62.

Magnuson, J. J. 1990. "Long-Term Ecological Research and the Invisible Present." *Bioscience* 40: 495–501.

Mammola, S., C. P. Carmona, T. Guillerme, and P. Cardoso. 2021. "Concepts and Applications in Functional Diversity." *Functional Ecology* 35: 1869–85.

McArdle, B. H., and M. J. Anderson. 2001. "Fitting Multivariate Models to Community Data: A Comment on Distance-Based Redundancy Analysis." *Ecology* 82: 290–97.

Médiène, S., M. Valantin-Morison, J.-P. Sarthou, S. De Tourdonnet, M. Gosme, M. Bertrand, J. Roger-Estrade, et al. 2011. "Agroecosystem Management and Biotic Interactions: A Review." *Agronomy for Sustainable Development* 31: 491–514.

Nohe, A., A. Goffin, L. Tyberghein, R. Lagring, K. De Cauwer, W. Vyverman, and K. Sabbe. 2020. "Marked Changes in Diatom and Dinoflagellate Biomass, Composition and Seasonality in the Belgian Part of the North Sea between the 1970s and 2000s." *Science of the Total Environment* 716: 136316.

Odum, E. P. 1950. "Bird Populations of the Highlands (North Carolina) Plateau in Relation to Plant Succession and Avian Invasion." *Ecology* 31: 587–605.

Ovaskainen, O., J. Rybicki, and N. Abrego. 2019. "What Can Observational Data Reveal about Metacommunity Processes?" *Ecography* 42: 1877–86.

Palacio, F. X., C. T. Callaghan, P. Cardoso, E. J. Hudgins, M. A. Jarzyna, G. Ottaviani, F. Riva, C. Graco-Roza, V. Shirey, and S. Mammola. 2022. "A Protocol for Reproducible Functional Diversity Analyses." *Ecography* 2022: e06287.

Park, J. S., and E. Post. 2022. "Seasonal Timing on a Cyclical Earth: Towards a Theoretical Framework for the Evolution of Phenology." *PLoS Biology* 20: e3001952.

Piao, S., Q. Liu, A. Chen, I. A. Janssens, Y. Fu, J. Dai, L. Liu, X. Lian, M. Shen, and X. Zhu. 2019. "Plant Phenology and Global Climate Change: Current Progresses and Challenges." *Global Change Biology* 25: 1922–40.

Piersma, T., and Å. Lindström. 2004. "Migrating Shorebirds as Integrative Sentinels of Global Environmental Change." *Ibis* 146: 61–69.

Poppeschi, C., G. Charria, A. Daniel, R. Verney, P. Rimmelin-Maury, M. Retho, E. Goberville, E. Grossteffan, and M. Plus. 2022. "Interannual Variability of the Initiation of the Phytoplankton Growing Period in Two French Coastal Ecosystems." *Biogeosciences* 19: 5667–87.

Post, E. 2019. *Time in Ecology: A Theoretical Framework*. Princeton, NJ: Princeton University Press.

Post, E., J. Kerby, C. Pedersen, and H. Steltzer. 2016. "Highly Individualistic Rates of Plant Phenological Advance Associated with Arctic Sea Ice Dynamics." *Biology Letters* 12: 20160332.

Quéguiner, B., and P. Tréguer. 1984. "Studies on the Phytoplankton in the Bay of Brest (Western Europe). Seasonal Variations in Composition, Biomass and Production in Relation to Hydrological and Chemical Features (1981–1982)." *Botanica Marina* 27: 449–460.

Ragueneau, O., B. Quéguiner, and P. Tréguer. 1996. "Contrast in Biological Responses to Tidally-Induced Vertical Mixing for Two Macrotidal Ecosystems of Western Europe." *Estuarine, Coastal and Shelf Science* 42: 645–665.

Ragueneau, O., M. Raimonet, C. Mazé, J. Coston-Guarini, L. Chauvaud, A. Danto, J. Grall, F. Jean, Y.-M. Paulet, and G.

Thouzeau. 2018. "The Impossible Sustainability of the Bay of Brest? Fifty Years of Ecosystem Changes, Interdisciplinary Knowledge Construction and Key Questions at the Science-Policy-Community Interface." *Frontiers in Marine Science* 5: 124.

Richardson, A. J., A. W. Walne, A. W. G. John, T. D. Jonas, J. A. Lindley, D. W. Sims, D. Stevens, and M. Witt. 2006. "Using Continuous Plankton Recorder Data." *Progress in Oceanography* 68: 27–74.

Ricotta, C. 2021. "From the Euclidean Distance to Compositional Dissimilarity: What Is Gained and What Is Lost." *Acta Oecologica* 111: 103732.

Rudolf, V. H. W. 2019. "The Role of Seasonal Timing and Phenological Shifts for Species Coexistence." *Ecology Letters* 22: 1324–38.

Sánchez-Pinillos, M., S. Kéfi, M. De Cáceres, and V. Dakos. 2023. "Ecological Dynamic Regimes: Identification, Characterization, and Comparison." *Ecological Monographs* 93: e1589.

Schwartz, M. D., ed. 2013. *Phenology: An Integrative Environmental Science*. Dordrecht: Springer Netherlands.

Steinberg, D. K., and M. R. Landry. 2017. "Zooplankton and the Ocean Carbon Cycle." *Annual Review of Marine Science* 9: 413–444.

Sturbois, A., J. Cucherousset, M. De Cáceres, N. Desroy, P. Riera, A. Carpentier, N. Quillien, et al. 2022. "Stable Isotope Trajectory Analysis (SITA): A New Approach to Quantify and Visualize Dynamics in Stable Isotope Studies." *Ecological Monographs* 92: e1501.

Sturbois, A., M. De Cáceres, A. Bifolchi, F. Bioret, A. Boyé, O. Gauthier, J. Grall, et al. 2023. "Ecological Quality Assessment: A Framework to Report Ecosystems Quality and Their Dynamics from Reference Conditions." *Ecosphere* 14: e4726.

Sturbois, A., M. De Cáceres, M. Sánchez-Pinillos, G. Schaal, O. Gauthier, P. L. Mao, A. Ponsero, and N. Desroy. 2021. "Extending Community Trajectory Analysis: New Metrics and Representation." *Ecological Modelling* 440: 109400.

Sturbois, A., and A. Ponsero. 2019. "Evolution des populations de limicoles et d'anatidés en baie de Saint-Brieuc." *Ornithos* 26: 232–243.

Sturbois, A., A. Ponsero, C. Jamet, N. Solsona, J. Petit, M. Plestan, O. Augé, Y. Février, and P. Yésou. 2024. "50 ans de suivi de l'avifaune sur la RNN de Saint-Brieuc: histoire, enseignement et responsabilités." *Ar Vran - Revue d'Ornithologie Bretonne* 31: 20–37.

Suding, K. N., S. Lavorel, F. S. Chapin Iii, J. H. C. Cornelissen, S. Díaz, E. Garnier, D. Goldberg, D. U. Hooper, S. T. Jackson, and M.-L. Navas. 2008. "Scaling Environmental Change through the Community-Level: A Trait-Based Response-and-Effect Framework for Plants." *Global Change Biology* 14: 1125–40.

Tett, P., C. Carreira, D. K. Mills, S. Van Leeuwen, J. Foden, E. Bresnan, and R. J. Gowen. 2008. "Use of a Phytoplankton Community Index to Assess the Health of Coastal Waters." *ICES Journal of Marine Science* 65: 1475–82.

Thornton, C., M. Panagiotopoulou, F. A. Chowdhury, B. Diehl, J. S. Duncan, S. J. Gascoigne, G. Besne, et al. 2024. "Diminished Circadian and Ultradian Rhythms of Human Brain Activity in Pathological Tissue In Vivo." *Nature Communications* 15: 8527.

Toumi, C., M. De Cáceres, J. Grall, A. Boyé, É. Thiébaut, M. Maguer, V. Le Garrec, C. Broudin, C. Houbin, and O. Gauthier. 2023. "Long-Term Coastal Macrobenthic Community Trajectory Analysis Reveals Habitat-Dependent Stability Patterns." *Ecography* 2023: e06489.

Tuomisto, H. 2010. "A Diversity of Beta Diversities: Straightening up a Concept Gone Awry. Part 2. Quantifying Beta Diversity and Related Phenomena." *Ecography* 33: 23–45.

Tye, S. P., S. B. Fey, J. P. Gibert, and A. M. Siepielski. 2024. "Predator Mass Mortality Events Restructure Food Webs Through Trophic Decoupling." *Nature* 626: 335–340.

Uriarte, I., F. Villate, A. Iriarte, Á. Fanjul, A. Atkinson, and K. Cook. 2021. "Opposite Phenological Responses of Zooplankton to Climate along a Latitudinal Gradient through the European Shelf." *ICES Journal of Marine Science* 78: 1090–1107.

van der Meer, J., T. Piersma, and J. J. Beukema. 2001. "Population Dynamics of Benthic Species on Tidal Flats: The Possible Roles of Shorebird Predation." In *Ecological Comparisons of Sedimentary Shores*, edited by K. Reise, 317–335. Berlin, Heidelberg: Springer Berlin Heidelberg.

Vellend, M. 2016. *The Theory of Ecological Communities*. Princeton, NJ: Princeton University Press.

Villéger, S., N. W. H. Mason, and D. Mouillot. 2008. "New Multidimensional Functional Indices for a Multifaceted Framework in Functional Ecology." *Ecology* 89: 2290–2301.

Weijerman, M., H. Lindeboom, and A. Zuur. 2005. "Regime Shifts in Marine Ecosystems of the North Sea and Wadden Sea." *Marine Ecology Progress Series* 298: 21–39.

White, E. R., and A. Hastings. 2020. "Seasonality in Ecology: Progress and Prospects in Theory." *Ecological Complexity* 44: 100867.

Wilson, R. J., N. S. Banas, M. R. Heath, and D. C. Speirs. 2016. "Projected Impacts of 21st Century Climate Change on Diapause in *Calanus finmarchicus*." *Global Change Biology* 22: 3332–40.

Wong, M. K. L., and R. K. Didham. 2024. "Global Meta-Analysis Reveals Overall Higher Nocturnal than Diurnal Activity in Insect Communities." *Nature Communications* 15: 3236.

Xiao, J., J. B. Fisher, H. Hashimoto, K. Ichii, and N. C. Parazoo. 2021. "Emerging Satellite Observations for Diurnal Cycling of Ecosystem Processes." *Nature Plants* 7: 877–887.

Yang, L. H. 2020. "Toward a more Temporally Explicit Framework for Community Ecology." *Ecological Research* 35: 445–462.

Zhao, C., U. Daewel, and C. Schrum. 2019. "Tidal Impacts on Primary Production in the North Sea." *Earth System Dynamics* 10: 287–317.

SUPPORTING INFORMATION

Additional supporting information can be found online in the Supporting Information section at the end of this article.

How to cite this article: Djeghri, Nicolas, Anthony Sturbois, Pierre Hélaouët, Quentin Geissmann, Peggy Rimmelin-Maury, Aurélien Boyé, Olivier Gauthier, and Miquel De Cáceres. 2026. "Going Round in Cycles but Going Somewhere: Deciphering Cyclical Dynamics Using Ecological Trajectory Analysis." *Ecological Monographs* 96(2): e70058. https://doi.org/10.1002/ecm.70058